

Clinical Imaging

Benign and malignant mimickers of infiltrative hepatocellular carcinoma: tips and tricks for differential diagnosis on CT and MRI

--Manuscript Draft--

Manuscript Number:	
Article Type:	Review Article
Keywords:	Hepatocellular carcinoma; Liver neoplasms; Differential diagnosis; Computed tomography; Magnetic Resonance Imaging
Corresponding Author:	Federica Vernuccio ITALY
First Author:	Federica Vernuccio
Order of Authors:	Federica Vernuccio Giorgia Porrello Roberto Cannella Laura Vernuccio Massimo Midiri Lydia Giannitrapani Maurizio Soresi Giuseppe Brancatelli
Abstract:	<p>Hepatocellular carcinoma (HCC) may have an infiltrative appearance in about 8-20% of cases. Infiltrative HCC can be a challenging diagnosis and it is associated with the worst overall survival among HCC patients. Infiltrative HCC is characterized by the spread of multiple minute nodules throughout the liver, without a dominant one, ultimately determining macrovascular invasion. On CT and MRI, infiltrative HCC appears as an ill-defined, large mass, with variable degree of enhancement, and satellite neoplastic nodules in up to 52% of patients. On MRI, it may show restriction on diffusion weighted imaging, hyperintensity on T2- and hypointensity on T1-weighted images, and, if hepatobiliary agent is used, hypointensity on hepatobiliary phase. Infiltrative HCC must be differentiated from other liver diseases, such as focal confluent fibrosis, steatosis, amyloidosis, vascular disorders of the liver, cholangiocarcinoma, and diffuse metastatic disease. In cirrhotic patients, the identification of vascular tumor invasion of the portal vein and its differentiation from bland thrombosis is of utmost importance for patient management. On contrast enhanced CT and MRI portal vein tumor thrombosis appears as an enhancing thrombus within the portal vein, close to the main tumor and determines vein enlargement. The aim of this pictorial review is to show CT and MRI features that allow the diagnosis of infiltrative HCC and portal vein tumor thrombosis. A particular point of interest includes the tips and tricks for differential diagnosis with potential mimickers of infiltrative HCC.</p>
Suggested Reviewers:	Kalina Chupetlovska k.chupetlovska@outlook.com Alessandro Furlan furlana@upmc.edu

Benign and malignant mimickers of infiltrative hepatocellular carcinoma: tips and tricks for differential diagnosis on CT and MRI

Federica Vernuccio, MD^{1,2,3,4}; Giorgia Porrello⁴, Roberto Cannella⁴, Laura Vernuccio⁵, Massimo Midiri⁴, Lydia Giannitrapani¹, Maurizio Soresi¹, Giuseppe Brancatelli⁴

1. Department of Health Promotion, Mother and Child Care, Internal Medicine and Medical Specialties (PROMISE),, University of Palermo, Palermo, Italy
2. University Paris Diderot, Sorbonne Paris Cité, Paris, France;
3. I.R.C.C.S. Centro Neurolesi Bonino Pulejo, Contrada Casazza, SS113, 98124 Messina
4. Department of Biomedicine, Neuroscience and Advanced Diagnostics (BIND), University Hospital of Palermo, Via del Vespro 129, 90127 Palermo, Italy.
5. U.O.C. Geriatria e Lungodegenza, AOUP University Hospital Palermo; CDCD Geriatria, University Hospital Palermo, Palermo .

Federica Vernuccio: federicavernuccio@gmail.com - federica.vernuccio@unipa.it

Giorgia Porrello: giorgia.porrello@gmail.com

Roberto Cannella: rob.cannella89@gmail.com

Laura Vernuccio: la.vernuccio@gmail.com

Massimo Midiri: massimo.midiri@unipa.it

Lydia Giannitrapani: lydiagiannitp@gmail.com

Maurizio Soresi: maurizio.soresi@unipa.it

Giuseppe Brancatelli: gbranca@yahoo.com

Corresponding Author: Federica Vernuccio, MD,
Radiologist, PhD Fellow
University of Palermo
Via del Vespro, 129
90127 - Palermo
Phone: +39 (388) 6332212
Email: federicavernuccio@gmail.com

Funding: None

Disclosures:

The authors have the following disclosures:

Federica Vernuccio: nothing to disclose for this study;

Giorgia Porrello: nothing to disclose for this study;

Roberto Cannella: nothing to disclose for this study;

Laura Vernuccio: nothing to disclose for this study;

Massimo Midiri: nothing to disclose for this study;

Lydia Giannitrapani: nothing to disclose for this study;

Maurizio Soresi: nothing to disclose for this study;

Giuseppe Brancatelli: nothing to disclose for this study.

Benign and malignant mimickers of infiltrative hepatocellular carcinoma: tips and tricks for differential diagnosis on CT and MRI

Pictorial Essay

Abstract

Hepatocellular carcinoma (HCC) may have an infiltrative appearance in about 8-20% of cases. Infiltrative HCC can be a challenging diagnosis and it is associated with the worst overall survival among HCC patients. Infiltrative HCC is characterized by the spread of multiple minute nodules throughout the liver, without a dominant one, ultimately determining macrovascular invasion. On CT and MRI, infiltrative HCC appears as an ill-defined, large mass, with variable degree of enhancement, and satellite neoplastic nodules in up to 52% of patients. On MRI, it may show restriction on diffusion weighted imaging, hyperintensity on T2- and hypointensity on T1-weighted images, and, if hepatobiliary agent is used, hypointensity on hepatobiliary phase. Infiltrative HCC must be differentiated from other liver diseases, such as focal confluent fibrosis, steatosis, amyloidosis, vascular disorders of the liver, cholangiocarcinoma, and diffuse metastatic disease. In cirrhotic patients, the identification of vascular tumor invasion of the portal vein and its differentiation from bland thrombosis is of utmost importance for patient management. On contrast enhanced CT and MRI portal vein tumor thrombosis appears as an enhancing thrombus within the portal vein, close to the main tumor and determines vein enlargement. The aim of this pictorial review is to show CT and MRI features that allow the diagnosis of infiltrative HCC and portal vein tumor thrombosis. A particular point of interest includes the tips and tricks for differential diagnosis with potential mimickers of infiltrative HCC.

26 **Keywords:** Hepatocellular carcinoma; Liver neoplasms; Differential diagnosis; Computed
1
27 tomography; Magnetic Resonance Imaging
3

4
28

6
29

8
9

10
11

12
13

14
15

16
17

18
19

20
21

22
23

24
25

26
27

28
29

30
31

32
33

34
35

36
37

38
39

40
41

42
43

44
45

46
47

48
49

50
51

52
53

54
55

56
57

58
59

60
61

62
63

64
65

1.0 Introduction

Hepatocellular carcinoma (HCC) is the fourth leading cause of cancer-related death worldwide according to the World Health Organization statistics, and it commonly arises in cirrhotic livers [1, 2]. HCC growth patterns can be categorized as nodular, massive or infiltrative at pathology [3, 4]. Each pattern behaves differently in regard to imaging diagnosis, response to treatment, disease progression and prognosis [3-7]. Whilst the nodular type represents the most common subtype, infiltrative HCC is the rarest one and accounts for approximately 8-20% of all HCC cases [2-8].

Infiltrative HCC arises more commonly in the setting of HBV or HBV+HCV co-infection and does not seem to be related to age nor duration of cirrhosis [7, 9]. This infiltrative growth pattern is characterized at pathology by the spread of multiple minute nodules without a dominant one [10], which translates on cross-sectional imaging into an ill-defined permeative mass that blends into the background cirrhotic parenchyma and makes the diagnosis challenging. Infiltrative HCC has an aggressive course and overall survival of around 10 months, which is even worse in case of vascular invasion of the portal vein [5-13]. Infiltrative HCC may mimic other benign and malignant entities, and, until now, there are no definitive imaging criteria to clearly differentiate between HCC with tumor in vein from other cancers with tumor invasion. Patients with infiltrative HCC tend to have worse liver function and elevated α -fetoprotein values ($>10,000$ ng/mL) with higher values as compared to patients with nodular HCC, although α -fetoprotein levels can be even normal or mildly elevated [6, 14].

The diagnosis of infiltrative HCC is also a therapeutic dilemma, as it narrows the therapeutic options in HCC patients [8, 11, 12, 15]. The European and American Association for the Study of Liver Diseases guidelines recommend systemic treatment with sorafenib as the treatment of choice [12, 16] and some studies also showed controversial results on the efficacy of intra-arterial therapies when non-extensive tumor thrombosis is

56 seen [11, 15]. Due to its aggressive nature and the high likelihood of vascular invasion and
1
27 extrahepatic metastatic disease, surgical resection and liver transplantation are not
3
4
58 recommended, due to the decreased survival expectations [8, 11-13]. Transarterial
6
79 radioembolization with Yttrium-90 is also considered a therapeutic option in patients with
8
9
60 infiltrative HCC, although survival results are still controversial [17, 18]. Finn et al [19] have
10
11
121 recently demonstrated that treatment with the combination of atezolizumab (i.e. a
13
14
62 programmed death ligand 1 inhibitor) and bevacizumab (i.e. a monoclonal antibody
15
16
173 targeting the vascular endothelial growth factor) results in significantly longer overall and
18
19
64 progression-free survival as well as strikingly better patient- reported outcomes than
20
21
225 sorafenib. Recent evidences also suggest that selected HCC patients with radiological
23
24
66 signs of vascular invasion could be considered for transplantation, provided that they
25
26
277 previously underwent successful treatment of the macrovascular invasion resulting in a
28
29
68 pretransplant α -fetoprotein < 10 ng/ml [20] and that selected patients diagnosed with HCC
30
31
69 and macrovascular invasion without extrahepatic metastasis may have better survival if
32
33
3470 treated with resection as compared to patients treated with sorafenib [21].
35

36
71 Therefore, knowledge of imaging clues for diagnosis of infiltrative HCC is of utmost
37
38
3972 importance for abdominal radiologists for a proper and prompt management. The aim of
40
41
73 this pictorial essay is to show CT and MRI features of infiltrative HCC and portal vein
42
43
4474 tumor thrombosis. A particular point of interest includes the tips and tricks for differential
45
46
75 diagnosis with potential mimickers of infiltrative HCC.
47
48
4976

50 5177 **1.2 CT and MRI Diagnosis of infiltrative HCC** 52

53
78 CT and MRI have a sensitivity of 62-72% and specificity of 88-95% for the diagnosis of
54
55
5679 nodular HCC, with values depending on technique, contrast agent, and tumor size [22].
57

58
80 The diagnosis of nodular HCC is quite straightforward when typical imaging features (i.e.
59
60
6181 size ≥ 10 mm, arterial phase hyperenhancement, washout on portal venous or delayed
62
63
64
65

82 phase, and enhancing capsule) are detected [23]. Conversely, infiltrative HCC lacks these
1
2
3
4
5
6
7
8
9
10
11
12
13
14
15
16
17
18
19
20
21
22
23
24
25
26
27
28
29
30
31
32
33
34
35
36
37
38
39
40
41
42
43
44
45
46
47
48
49
50
51
52
53
54
55
56
57
58
59
60
61
62
63
64
65

typical imaging features, and thus represents a diagnostic conundrum [6, 11]. In some cases, HCC is not visible and the only clue to the diagnosis may be neoplastic portal vein thrombosis [7]

CT and MRI features that suggest the diagnosis of infiltrative HCC are the presence of an ill-defined mass, usually larger than nodular HCC and without fibrotic margins, with minimal or inconsistent arterial enhancement, heterogeneous washout appearance on portal venous or delayed phases, and malignant portal vein tumor thrombosis (**Figure 1**) [7, 10,11, 24-27].

The minimal or inconsistent arterial enhancement in infiltrative HCC may be due to both the infiltrative nature of the tumor and the presence of portal vein thrombosis, which results in perfusion changes that can conceal the tumor on dynamic phases; therefore, sometimes the tumor is not visible and malignant portal vein thrombosis is the only sign of infiltrative HCC [7, 10, 27-30]. CT and MRI diagnosis of malignant portal vein thrombosis in infiltrative HCC is based on the presence of thrombus neovascularity which corresponds to the “thread and streak sign” in angiography (i.e. a thin linear or chainlike opacification in the portal vein during early hepatic arteriography) (**Figure 2**) [13, 31], portal vein expansion (i.e. main portal vein diameter greater than or equal to 23 mm is highly specific) [32] and proximity to the main tumor or direct neoplastic portal invasion [25, 33, 34]. In case of extensive portal vein invasion, infiltrative HCC-associated thrombosis can fill the peripheral portal vein branches, creating a dilated tumor-filled “cast” of these vessels [7].

MRI allows to appreciate the tumor as homogeneously or heterogeneously hypointense on T1-weighted images, mild to moderately hyperintense on T2-weighted images, and hyperintense, compared with surrounding liver parenchyma, on diffusion-weighted images with high b values ($b = 500\text{--}800 \text{ sec/mm}^2$) due to the tightly packed cellular arrangement, with corresponding low signal on apparent diffusion coefficient (ADC) map [10, 11, 24-27,

108 30, 35, 36]. The use of hepatobiliary MRI contrast agents can provide additional clues for
1
109 the diagnosis of infiltrative HCC, showing a reticular hypointense appearance on
2
3
4
110 transitional and hepatobiliary phases [10, 11, 30] and has demonstrated higher sensitivity
5
6
111 compared to contrast enhanced CT [37].
7
8
9

112 **1.3 Mimickers of infiltrative HCC: tips and tricks for differential diagnosis**

113
114 Many benign and malignant focal lesions may mimic infiltrative HCC and tumor thrombosis
15
115 on CT and MRI. The differential diagnosis is mandatory due to the different management
16
17 and prognosis. **Figure 3** summarize the main mimickers of infiltrative HCC and imaging
18
19 findings that help in the differential diagnosis with infiltrative HCC. Considering that
20
21 infiltrative HCC develops predominantly in cirrhotic liver, we differentiate the benign
22
23 mimickers based on the presence or lack of cirrhosis. With regard to malignant mimickers,
24
25 HCC has a higher incidence on cirrhotic liver as compared to healthy liver, whilst other
26
27 malignancies usually occur in the setting of non-cirrhotic liver, but may mimic infiltrative
28
29 HCC in some cases.
30
31
32
33
34
35

36 **1.4 Benign entities in cirrhotic liver**

37 *1.4.1 Focal Confluent Fibrosis*

38
39 Focal confluent fibrosis is a benign entity that may be identified in patients with long-
40
41 standing cirrhosis [38]. On CT and MRI, both infiltrative HCC and focal confluent fibrosis
42
43 show low attenuation or intensity compared to normal liver on noncontrast CT and T1-
44
45 weighted images, with minimal or inconsistent arterial enhancement, and mild-to-moderate
46
47 hyperintensity on T2-weighted sequences [10, 26, 38]. However, focal confluent fibrosis
48
49 has some distinctive imaging features that allow a confident diagnosis, including the
50
51 location (typically in segments 8 and 4), the peripheral, focal, wedge-shaped appearance
52
53
54
55
56
57
58
59
60
61
62
63
64
65

134 with capsular retraction, and the progressive enhancement on delayed extracellular
1
135 phases (**Figure 4**) [26, 38]. Conversely, the acquisition of the hepatobiliary phase usually
2
3
4
136 does not provide any tips for the differential diagnosis because both conditions lack the
5
6
137 ability to uptake contrast agent [10, 26].
7
8

9
10
11
12
13
14
15
16
17
18
19
20
21
22
23
24
25
26
27
28
29
30
31
32
33
34
35
36
37
38
39
40
41
42
43
44
45
46
47
48
49
50
51
52
53
54
55
56
57
58
59
60
61
62
63
64
65

1.4.2 Bland Thrombosis

Cirrhotic patients may develop benign portal vein thrombosis due to portal hypertension and stasis [13, 32-34], and this bland thrombosis may be erroneously interpreted as vascular tumor invasion of the portal vein occurring in infiltrative HCC. Arterial phase plays a pivotal role for the differentiation between bland (**Figure 5**) and malignant (**Figure 2**) portal thrombosis [27]. **Figure 6** summarizes the key differences between bland and malignant portal vein thrombosis. Compared to bland thrombosis, malignant tumor thrombus shows more commonly thrombus enhancement (100% versus 8.5%), venous expansion (91.7% versus 10.6%), neovascularity (58.3% versus 2.1%), and is adjacent to HCC or prior treatment site (100% versus 21.3%) [14]. MRI is also useful because malignant tumor thrombosis may show restricted diffusion on diffusion-weighted images and subtle T2 hyperintense signal [7, 27, 30]. In cirrhotic patients, the differential diagnosis between bland thrombosis and HCC infiltrating the portal vein has an important clinical impact because bland thrombosis may regress after anticoagulant therapy, while HCC with portal vein invasion requires systemic therapy in the form of sorafenib and thrombosis may occasionally regress after this therapy (**Figure 7**) [12, 16; 39].

1.5 Benign entities in non-cirrhotic liver

1.5.1 Acute Hepatitis

159 Acute hepatitis is a clinical diagnosis characterized by acute inflammation or injury to
1
160 hepatocytes, resulting in fever, abdominal pain, jaundice, and elevation of liver
2
3
4
161 biochemical lab tests. The cause of the injury may be viral (e.g. acute viral hepatitis A) or
5
6
162 non-viral (e.g. drug-induced, alcoholic, or autoimmune acute hepatitis) [40]. Whilst normal
7
8
163 imaging appearance of the liver does not exclude the diagnosis, CT and MRI features of
9
10
11
164 acute hepatitis may include hepatomegaly, periportal edema (e.g. decreased attenuation
12
13
14
165 on CT and increased T2 signal on MRI around the portal system and at the hepatic hilum),
15
16
166 diffusely decreased parenchymal attenuation on noncontrast CT corresponding to areas of
17
18
19
167 mild generalized increase in parenchymal signal intensity on T2-weighted and decreased
20
21
22
168 signal intensity on T1-weighted images, and occasionally areas of steatosis on dual-phase
23
24
169 sequence (**Figure 8**) [41-43]. On post-contrast CT and MRI, heterogeneous enhancement
25
26
170 and ill-defined regions of reduced enhancement may be present with reduced uptake of
27
28
29
171 hepatobiliary contrast agents and may simulate infiltrative HCC. The acute clinical onset,
30
31
172 the presence of periportal edema, gallbladder wall thickening, and the reversibility of the
32
33
34
173 heterogenous enhancement with improvement of liver function are useful tips for
35
36
174 differential diagnosis [41-45]. Imaging findings of acute hepatitis are nonspecific and final
37
38
175 diagnosis is clinically made.
39
40

41 42 43 44 1.5.2 Metabolic and Storage Diseases: Steatosis, Sarcoidosis and Amyloidosis

45
46
178 Metabolic and storage diseases are characterized by accumulation of storage material
47
48
179 within the liver. Among these, steatosis, sarcoidosis and amyloidosis are benign liver
49
50
51
180 conditions characterized by deposition of fat, inflammatory cells and amyloid within hepatic
52
53
181 parenchyma, respectively.
54

55
56
182 Fat deposition with geographic distribution shows low attenuation on noncontrast CT and
57
58
183 may have ill-defined margins, therefore potentially mimicking infiltrative HCC. However,
59
60
184 the signal drop on opposed-phase compared to the in-phase images, the lack of mass
61
62
63
64
65

185 effect on vessels and biliary ducts, the presence of undistorted vessels traversing through
1
186 the area of focal steatosis (**Figure 9**), and the incidental diagnosis in otherwise healthy
2
3
4
187 patients are useful tips for the differential diagnosis [10, 46].
5
6

188 Hepatic sarcoidosis is characterized by the presence of multiple small granulomatous
7
8
189 lesions, scattered throughout the liver with involvement mainly of portal and periportal
9
10
11
190 zones of hepatic lobules, that may lead to progressive interlobular bile duct injury with
12
13
14
191 cholestasis, fibrosis of portal tracks and, rarely, evolves into cirrhosis and portal
15
16
192 hypertension [47]. The occurrence of such multiple tiny poorly defined heterogenous
17
18
19
193 nodules – most of which are less than 1 cm in size – may simulate the presence of an
20
21
194 infiltrative HCC on post-contrast images (**Figure 10**), particularly when the liver has a
22
23
195 cirrhotic morphology. MRI finding of hepatic sarcoidosis include the identification of
24
25
196 granulomatous nodules as hypointense on both T1- and T2-weighted sequences [48] with
26
27
28
197 hypointense periportal areas on T2-weighted images (also known as T2 halo sign) that
29
30
31
198 show poor enhancement on post-contrast images [49]. In rare cases, the granulomatous
32
33
199 lesions may coalesce and imaging demonstrates large confluent hepatic lesions [50, 51].
34
35
200 Some of the tips that may help point towards a diagnosis of sarcoidosis include the
36
37
38
201 patency of portal vein branches, the presence of concomitant splenic granulomas, and the
39
40
202 identification of typical chest imaging features.
41
42

203 Hepatic amyloidosis is a rare infiltrative disease affecting the hepatic parenchyma
43
44
45
204 characterized by deposition of amyloid within the space of Disse along the sinusoids or
46
47
48
205 along the blood vessel walls that may lead to compression and near disappearance of
49
50
206 hepatocytes. The infiltrative appearance of amyloidosis may simulate infiltrative HCC. CT
51
52
207 and MRI findings of hepatic amyloidosis include hepatomegaly, heterogeneously
53
54
55
208 decreased parenchymal attenuation on noncontrast CT, and focal hypoattenuating areas
56
57
209 on post-contrast phases (**Figure 11**) – probably related to impaired blood flow – that tend
58
59
60
61
62
63
64
65

210 to homogenize on delayed images [52]. However, imaging findings are nonspecific and
1
211 final diagnosis is made at pathology.

212

213

213 1.5.3 Vascular Diseases of the Liver

214

214 Vascular diseases of the liver are rare conditions that affect the hepatic vascular system at
10
11 a presinusoidal (e.g. Rendu-Osler-Weber disease, portal vein thrombosis, extrinsic
1215 compression of portal vein, aneurysmal dilatation of the portal vein, sclerosing granulomas
13
1416 due to schistosomiasis, sarcoidosis or tuberculosis), intrasinusoidal (i.e. chronic hepatitis,
15
1617 cirrhosis, peliosis hepatis, or storage of substances such as fatty liver or amyloidosis) or
18
1918 post-sinusoidal (e.g. Budd-Chiari syndrome, sinusoidal obstruction syndrome, right heart
20
2119 failure) level [53, 54]. Regardless of the location, the obstacle in the hepatic vascular
22
2320 system leads to changes of hepatic parenchymal enhancement that may simulate the
24
2521 presence of an infiltrative HCC.
26
2722

223

223 Portal vein thrombosis has been discussed above among the benign entities in cirrhotic
31
3224 liver. Among the other vascular diseases of the liver, Rendu-Osler-Weber disease and
33
3425 Budd-Chiari syndrome will be discussed below as examples.
35
3626

227

227 Rendu-Osler-Weber disease, also known as hereditary hemorrhagic telangiectasia is
37
3840 characterized by widespread cutaneous, mucosal and visceral arteriovenous
3927 malformations that can involve lung, brain, or liver [53]. Specifically, liver vascular
41
4228 malformations range from tiny telangiectases to discrete arteriovenous malformations
43
4429 including arteriovenous, portovenous, and arterioportal shunts. Imaging features of Rendu-
45
4630 Osler-Weber disease include a transient mosaic type heterogeneous perfusion pattern of
47
4831 the liver in the arterial phase due to multiple arteriovenous shunts and telangiectases that
49
5032 is no longer seen in the portal venous phase (**Figure 12**), hepatic artery, hepatic vein and
51
5233 portal vein dilatation, opacification of the hepatic veins in the arterial phase in case of
53
5434 hepatic arteriosystemic venous shunt and, occasionally, FNH lesions [53, 55, 56].
55
5635

235

236

237

238

239

240

236 Budd-Chiari syndrome is a vascular liver disorder related to a hepatic venous outflow
1
237 obstruction at the level of the hepatic veins or at the junction of the inferior vena cava and
3
4
238 right atrium. In the acute phase of the disease, CT and MRI findings include heterogenous
5
6
239 liver enhancement (**Figure 13**) characterized by decreased enhancement on arterial
8
9
240 phase of more congested peripheral liver and increased enhancement of central portion of
10
11
241 the liver [57]. In subacute and chronic phases, some of the CT and MR imaging features
13
14
242 include focal nodular hyperplasia-like lesions, peripheral hepatic atrophy with
15
16
243 compensatory hypertrophy of the central regions, and irregular hepatic contour due to
18
19
244 fibrosis [57]. Useful tips that should prompt towards the diagnosis of Budd-Chiari
20
21
245 syndrome include the occurrence in young women, the “nutmeg” appearance on contrast
23
246 enhanced CT and MRI, the identification of occlusion of hepatic veins or inferior vena cava
25
26
247 but patency of portal vein, the presence of intra- or extra-hepatic collateral circulation
28
248 bypassing venous obstruction (which indicates a chronic process), and the splenic
30
31
249 involvement if the etiology is a hematological disorder [53, 54, 57].
32

33
34
35

36 **1.6 Malignant mimickers of infiltrative HCC**

37

38
39
40

41 *1.6.1 Intrahepatic Cholangiocarcinoma*

42

43 Intrahepatic cholangiocarcinoma can appear as ill-defined, large masses with low
44
45 attenuation or intensity on noncontrast CT or T1-weighted images and hyperintensity on
46
47 T2-weighted images [10, 58], and can mimic infiltrative HCC. Nonetheless,
48
49
50
51
52
53
54
55
56
57
58
59
60
61
62
63
64
65

262 causes an encasement of the vessels without definitive tumor thrombosis, a radiological
1
263 sign that is helpful for differential diagnosis with HCC. However, it is important to know
2
3
4
264 that, although rarely, cholangiocarcinoma with intravascular tumor thrombosis is possible
5
6
265 **(Figure 14)**.
7
8
9

10 11 1267 *1.6.2 Lymphoma* 13

14
1568 Hepatic lymphoma is uncommon and broadly includes secondary hepatic involvement
16
1269 (most common) and primary hepatic lymphoma, which is extremely rare. Hepatic
17
18
1970 lymphoma may present with multifocal lesions or diffuse infiltration or as an ill-defined
20
21
2271 mass in the porta hepatis in up to 90% of cases of secondary hepatic involvement, and in
23
2472 about 35% of cases of primary hepatic lymphoma (indicating a poor prognosis). This
25
26
2773 presentation of hepatic lymphoma may potentially simulate infiltrative HCC considering
28
2974 that both these entities may occur in patients who have cirrhosis with viral hepatitis [59,
30
31
3275 60]. In case of multifocal lesions, lymphomatous nodules are usually multiple with variable
33
3476 size and show hypoattenuation on non-contrast CT, hypointense on T1- and hyperintense
35
3677 on T2-weighted images and commonly enhance to a lesser degree than the liver
37
38
3978 parenchyma on all post-contrast phases **(Figure 16)** [60-63]. Lymphomatous infiltration of
40
4179 tumour cells into the portal tracts as well as sinusoids may demonstrate
42
43
4480 hepatosplenomegaly and subtle T2-hyperintensity with diffusion restriction **(Figure 15)**,
45
4681 findings that can be also detected in patients with infiltrative HCC [61-64]. Some tips that
47
48
4982 favour the diagnosis of hepatic lymphoma include the normal levels of α -fetoprotein, the
50
5183 presence of lymphadenopathies below the level of the renal veins, and the presence of
52
53
5484 vascular encasement without thrombosis [60, 61, 64, 65].
55
5685

57 5886 *1.6.3 Diffuse Metastatic Disease* 59 60 61 62 63 64 65

287 Hepatic metastases usually present as discrete nodules, with ring enhancement on post-
1
288 contrast phases. Less commonly, liver metastases show a diffuse metastatic spread with
2
3
4
289 an infiltrative appearance mimicking infiltrative HCC [66-68]. The clinical relevance of its
5
6
290 prompt recognition is particularly related to the potential acute hepatic failure related to the
7
8
291 diffuse intrasinusoidal spread of the hepatic metastases [66-69]. Indeed, as demonstrated
9
10
11
122 at pathology, neoplastic cells diffusely infiltrate the hepatic sinusoids, invade branches of
13
14
293 the hepatic and portal veins, and, as a consequence of pressure atrophy or vascular
15
16
1294 infarction, hepatocytes may be destroyed resulting in liver failure and a rapidly fatal course
17
18
19
295 [69]. The absence of classic discrete tumor masses may lead to underestimation of the
20
21
2296 tumor burden on CT and MRI [68]. CT and MRI may reveal multiple ill-defined masses
22
23
2297 scattered throughout the liver, hypovascular on post-contrast phases and being
24
25
26
298 demonstrated as diffuse small high-intensity areas on T2-weighted images and diffuse
27
28
2299 weighted images [66].
29
30

300 Pseudocirrhosis may occur in patients with liver metastases as a response to
31
32
33
301 chemotherapy and may also lead to portal hypertension that may regress completely after
34
35
36
302 chemotherapy discontinuation [70,71]. Although both pseudocirrhosis with diffuse
37
38
303 metastases and infiltrative HCC can present with a cirrhotic-shaped liver with multiple
39
40
41
404 hepatic lesions with low attenuation or intensity on noncontrast CT or T1-weighted images,
42
43
405 hyperintense on T2-weighted images, as well as restricted diffusion on diffusion weighted
44
45
406 imaging (**Figure 16**) [72], the clinical setting (e.g. presence of known primary malignancy,
46
47
48
307 history of cirrhosis, elevated levels of alpha fetoprotein or other tumor markers) and the
49
50
508 typical rim-enhancing pattern of liver metastases on post-contrast phases allow a confident
51
52
53
309 diagnosis.
54
55

56 57 58 **1.7 Summary** 59

60
61
62
63
64
65

312 The diagnosis of infiltrative HCC and its eventually associated neoplastic thrombosis may
1
313 be challenging. Considering the poor prognosis of infiltrative HCC and the different
3
4
314 management of infiltrative HCC and tumor thrombosis as compared to nodular HCC and
5
6
315 bland thrombosis, abdominal radiologists are required to know CT and MRI features of
7
8
316 infiltrative HCC and the tips and tricks for the differential diagnosis with its mimickers.
9
10
11
12
13
14
15
16
17
18
19
20
21
22
23
24
25
26
27
28
29
30
31
32
33
34
35
36
37
38
39
40
41
42
43
44
45
46
47
48
49
50
51
52
53
54
55
56
57
58
59
60
61
62
63
64
65

318
1
319
3
4
320
6
321
8
9
322
10
11
323
13
14
324
15
16
325
18
19
326
20
21
327
23
24
328
25
26
329
27
28
330
30
31
331
32
33
332
35
36
333
37
38
334
40
41
335
42
43
336
44
45
46
337
47
48
338
49
50
51
339
52
53
340
54
55
56
341
57
58
342
59
60
343
61
62
63
64
65

References

1. Siegel RL, Miller KD, Jemal A. Cancer statistics, 2019. *CA Cancer J Clin.* 2019; 69:7–34.
2. Ferlay J, Soerjomataram I, Ervik M, Dikshit R, Eser S, Mathers C et al. GLOBOCAN 2012 v1.0, Cancer Incidence and Mortality Worldwide: IARC CancerBase No. 11. Lyon, France: International Agency for Research on Cancer; 2013.
3. Trevisani F, Caraceni P, Bernardi M, D’Intino PE, Arienti V, Amorati P, et al. Gross pathologic types of hepatocellular carcinoma in Italian patients. Relationship with demographic, environmental, and clinical factors. *Cancer.* 1993; 72:1557–1563.
4. Kojiro M. Histopathology of liver cancers. *Best Pract Res Clin Gastroenterol* 2005;19:39–62.
5. He J, Shi J, Fu X, Mao L, Zhou T, Qiu Y, et al. The Clinicopathologic and Prognostic Significance of Gross Classification on Solitary Hepatocellular Carcinoma After Hepatectomy. *Medicine (Baltimore).* 2015 Aug;94(32):e1331. doi: 10.1097/MD.0000000000001331.
6. Yopp AC, Mokdad A, Zhu H, Mansour JC, Balch GC, Choti MA, et al. Infiltrative Hepatocellular Carcinoma: Natural History and Comparison with Multifocal, Nodular Hepatocellular Carcinoma. *Ann Surg Oncol.* 2015;22 Suppl 3:S1075-82. doi: 10.1245/s10434-015-4786-7.
7. Demirjian A, Peng P, Geschwind JF, Cosgrove D, Schutz J, Kamel IR, et al. Infiltrating hepatocellular carcinoma: seeing the tree through the forest. *J Gastrointest Surg.* 2011;15(11):2089-97. doi: 10.1007/s11605-011-1614-7.
8. Dendy MS, Camacho JC, Ludwig JM, Krasinskas AM, Knechtle SJ, Kim HS. Infiltrative Hepatocellular Carcinoma With Portal Vein Tumor Thrombosis Treated With a Single High-Dose Y90 Radioembolization and Subsequent Liver

344 Transplantation Without a Recurrence. *Transplant Direct*. 2017;3(9):e206. doi:
1 10.1097/TXD.0000000000000707.
345 10.1097/TXD.0000000000000707.
3 4
346 9. Benvegnù L, Noventa F, Bernardinello E, Pontisso P, Gatta A, Alberti A. Evidence
6 for an association between the aetiology of cirrhosis and pattern of hepatocellular
347 carcinoma development. *Gut*. 2001;48(1):110-5. doi: 10.1136/gut.48.1.110.
8 9
348 10. Reynolds AR, Furlan A, Fetzer DT, Sasatomi E, Borhani AA, Heller MT, et al.
10 Infiltrative hepatocellular carcinoma: what radiologists need to know. *Radiographics*.
11 2015;35(2):371-86. doi: 10.1148/rg.352140114.
12 13
14 11. Kneuertz PJ, Demirjian A, Firoozmand A, Corona-Villalobos C, Bhagat N, Herman
15 J, et al. Diffuse infiltrative hepatocellular carcinoma: assessment of presentation,
16 treatment, and outcomes. *Ann Surg Oncol*. 2012; 19:2897-907. doi:
17 10.1245/s10434-012-2336-0..
18 19
20 12. EASL - European Association for the Study of the Liver, Clinical Practice
21 Guidelines: Management of hepatocellular carcinoma. *J Hepatol*. 2018; 69:182-236.
22 doi: 10.1016/j.jhep.2018.03.019. Erratum in: *J Hepatol*. 2019;70:817.
23 24
25 13. Canellas R, Mehrkhani F, Patino M, Kambadakone A, Sahani D. Characterization of
26 Portal Vein Thrombosis (Neoplastic Versus Bland) on CT Images Using Software-
27 Based Texture Analysis and Thrombus Density (Hounsfield Units). *American
28 Journal of Roentgenology*. 2016; 207:W81-W87. doi:10.2214/AJR.15.15928
29 30
31 14. Sherman CB, Behr S, Dodge JL, Roberts JP, Yao FY, Mehta N. Distinguishing
32 Tumor From Bland Portal Vein Thrombus in Liver Transplant Candidates With
33 Hepatocellular Carcinoma: the A-VENA Criteria. *Liver Transpl*. 2019; 25:207-216.
34 doi:10.1002/lt.25345.
35 36
37 15. Lopez RR Jr, Pan SH, Hoffman AL, Ramirez C, Rojter SE, Ramos H, et al.
38 Comparison of transarterial chemoembolization in patients with unresectable,
39
40
41
42
43
44
45
46
47
48
49
50
51
52
53
54
55
56
57
58
59
60
61
62
63
64
65

- 369 diffuse vs focal hepatocellular carcinoma. Arch Surg. 2002;137:653-7; discussion
1
370 657-8. doi: 10.1001/archsurg.137.6.653.
3
4
371 16. Heimbach JK, Kulik LM, Finn RS, Sirlin CB, Abecassis MM, Roberts LR, Zhu AX,
6
372 Murad MH, Marrero JA. AASLD guidelines for the treatment of hepatocellular
8
373 carcinoma. Hepatology. 2018; 67:358-380. doi: 10.1002/hep.29086.
10
11
374 17. Sposito C, Mazzaferro V. The SIRveNIB and SARA trials, radioembolization vs.
13
375 sorafenib in advanced HCC patients: reasons for a failure, and perspectives for the
14
15
16
376 future. Hepatobiliary Surg Nutr. 2018; 7:487-489. doi:10.21037/hbsn.2018.10.06
18
19
377 18. Spreafico C, Sposito C, Vaiani M, Cascella T, Bhoori S, Morosi C, et al.
20
21
378 Development of a prognostic score to predict response to Yttrium-90
23
379 radioembolization for hepatocellular carcinoma with portal vein invasion. J Hepatol.
25
26
380 2018; 68:724-732. doi: 10.1016/j.jhep.2017.12.026.
28
29
381 19. Finn RS, Qin S, Ikeda M, Galle PR, Ducreux M, Kim TY, et al. Atezolizumab plus
30
31
382 Bevacizumab in Unresectable Hepatocellular Carcinoma. N Engl J Med. 2020;
32
33
383 382:1894-1905. doi: 10.1056/NEJMoa1915745.
35
36
384 20. Assalino M, Terraz S, Grat M, Lai Q, Vachharajani N, Gringeri E, et al. Liver
37
38
385 transplantation for hepatocellular carcinoma after successful treatment of
40
41
386 macrovascular invasion - a multi-center retrospective cohort study. Transpl Int.
42
43
387 2020; 33:567-575. doi: 10.1111/tri.13586.
45
46
388 21. Mei J, Li SH, Wang QX, Lu LH, Ling YH, Zou JW, et al. Resection vs. Sorafenib for
47
48
389 Hepatocellular Carcinoma With Macroscopic Vascular Invasion: A Real World,
49
50
390 Propensity Score Matched Analytic Study. Front Oncol. 2020;10:573. doi:
52
53
391 10.3389/fonc.2020.00573.
54
55
392 22. Lee S, Kim SS, Roh YH, Choi JY, Park MS, Kim MJ. Diagnostic Performance of
57
58
393 CT/MRI Liver Imaging Reporting and Data System v2017 for Hepatocellular
59
60
61
62
63
64
65

394 Carcinoma: A Systematic Review and Meta-Analysis. *Liver Int.* 2020; 40:1488-
1
395 1497.

396 23. ACR CEUS LI-RADS® v2017. (last access on 20/04/2020)

397 24. Kanematsu M, Semelka RC, Leonardou P, Mastropasqua M, Lee JK.

398 Hepatocellular carcinoma of diffuse type: MR imaging findings and clinical
10
11
12
13
14
15
16
17
18
19
20
21
22
23
24
25
26
27
28
29
30
31
32
33
34
35
36
37
38
39
40
41
42
43
44
45
46
47
48
49
50
51
52
53
54
55
56
57
58
59
60
61
62
63
64
65
manifestations. *J Magn Reson Imaging.* 2003; 18:189-95. doi: 10.1002/jmri.10336.

400 25. Kim YK, Han YM, Kim CS. Comparison of diffuse hepatocellular carcinoma and
15
16
17
18
19
20
21
22
23
24
25
26
27
28
29
30
31
32
33
34
35
36
37
38
39
40
41
42
43
44
45
46
47
48
49
50
51
52
53
54
55
56
57
58
59
60
61
62
63
64
65
intrahepatic cholangiocarcinoma using sequentially acquired gadolinium-enhanced
and Resovist-enhanced MRI. *Eur J Radiol.* 2009; 70:94-100.

403 26. Park YS, Lee CH, Kim BH, Lee J, Choi JW, Kim KA, et al. Using Gd-EOB-DTPA-
23
24
25
26
27
28
29
30
31
32
33
34
35
36
37
38
39
40
41
42
43
44
45
46
47
48
49
50
51
52
53
54
55
56
57
58
59
60
61
62
63
64
65
enhanced 3-T MRI for the differentiation of infiltrative hepatocellular carcinoma and
focal confluent fibrosis in liver cirrhosis. *Magn Reson Imaging.* 2013; 31:1137-42.
doi: 10.1016/j.mri.2013.01.011.

407 27. Lim S, Kim YK, Park HJ, Lee WJ, Choi D, Park MJ. Infiltrative hepatocellular
32
33
34
35
36
37
38
39
40
41
42
43
44
45
46
47
48
49
50
51
52
53
54
55
56
57
58
59
60
61
62
63
64
65
carcinoma on gadoxetic acid-enhanced and diffusion-weighted MRI at 3.0T. *J Magn
Reson Imaging.* 2014; 39:1238-45. doi: 10.1002/jmri.24265.

410 28. Thian YL, Low AS, Chow PK, Ooi LL, Chung AY, Low SC, Xie W, Thng CH.

411 Atypical enhancement pattern of hepatocellular carcinoma with portal vein
42
43
44
45
46
47
48
49
50
51
52
53
54
55
56
57
58
59
60
61
62
63
64
65
thrombosis on multiphasic CT. *Ann Acad Med Singapore.* 2011;40:454-9.

413 29. Danila M, Sporea I, Popescu A, Şirli R. Portal vein thrombosis in liver cirrhosis - the
47
48
49
50
51
52
53
54
55
56
57
58
59
60
61
62
63
64
65
added value of contrast enhanced ultrasonography. *Med Ultrason.* 2016;18:218-33.
doi: 10.11152/mu.2013.2066.182.pvt.

416 30. Rosenkrantz AB, Lee L, Matza BW, Kim S. Infiltrative hepatocellular carcinoma:
54
55
56
57
58
59
60
61
62
63
64
65
comparison of MRI sequences for lesion conspicuity. *Clin Radiol.* 2012; 67:e105-11.
doi: 10.1016/j.crad.2012.08.019.

- 419 31. Raab BW. The thread and streak sign. *Radiology*. 2005; 236:284-5.
1
2
420 doi:10.1148/radiol.2361030114
3
4
421 32. Tublin ME, Dodd GD 3rd, Baron RL. Benign and malignant portal vein thrombosis:
5
6
422 differentiation by CT characteristics. *AJR Am J Roentgenol*. 1997; 168:719-23.
7
8
423 doi:10.2214/ajr.168.3.9057522
9
10
11
424 33. Piscaglia F, Gianstefani A, Ravaioli M, Golfieri R, Cappelli A, Giampalma E, et al.
12
13
425 Criteria for diagnosing benign portal vein thrombosis in the assessment of patients
14
15
426 with cirrhosis and hepatocellular carcinoma for liver transplantation. *Liver Transpl*.
16
17
427 2010; 16:658-67. doi: 10.1002/lt.22044.
18
19
20
21
428 34. Margini C, Berzigotti A. Portal vein thrombosis: The role of imaging in the clinical
22
23
429 setting. *Dig Liver Dis*. 2017;49(2):113–20. doi:10.1016/j.dld.2016.11.013
24
25
26
430 35. Choi JY, Lee JM, Sirlin CB. CT and MR imaging diagnosis and staging of
27
28
431 hepatocellular carcinoma: part II. Extracellular agents, hepatobiliary agents, and
29
30
432 ancillary imaging features. *Radiology*. 2014;273:30-50. doi:
31
32
433 10.1148/radiol.14132362.
33
34
35
434 36. Yu NC, Chaudhari V, Raman SS, Lassman C, Tong MJ, Busuttill RW, et al. CT and
36
37
435 MRI improve detection of hepatocellular carcinoma, compared with ultrasound
38
39
40
436 alone, in patients with cirrhosis. *Clin Gastroenterol Hepatol*. 2011; 9:161-7. doi:
41
42
43
437 10.1016/j.cgh.2010.09.017.
44
45
438 37. Bae JS, Lee JM, Yoon JH, Jang S, Chung JW, Lee KB, et al. How to Best Detect
46
47
439 Portal Vein Tumor Thrombosis in Patients with Hepatocellular Carcinoma Meeting
48
49
50
440 the Milan Criteria: Gadoteric Acid-Enhanced MRI versus Contrast-Enhanced CT.
51
52
441 *Liver Cancer*. 2020; 9:293-307. doi: 10.1159/000505191.
53
54
55
442 38. Brancatelli G, Baron RL, Federle MP, Sparacia G, Pealer K. Focal confluent fibrosis
56
57
443 in cirrhotic liver: natural history studied with serial CT. *AJR Am J Roentgenol*. 2009;
58
59
444 192:1341-7. doi: 10.2214/AJR.07.2782.
60
61
62
63
64
65

- 445 39. Bruix J, Sherman M; American Association for the Study of Liver Diseases.
1
446 Management of hepatocellular carcinoma: an update. *Hepatology*. 2011; 53:1020-2.
3
447 doi: 10.1002/hep.24199.
6
- 448 40. Ryder SD, Beckingham IJ. ABC of diseases of liver, pancreas, and biliary system:
8
449 Acute hepatitis. *BMJ*. 2001; 322:151-3. doi: 10.1136/bmj.322.7279.151.
10
- 450 41. Park SJ, Kim JD, Seo YS, Park BJ, Kim MJ, Um SH, et al. Computed tomography
13
451 findings for predicting severe acute hepatitis with prolonged cholestasis. *World J*
15
452 *Gastroenterol*. 2013; 19:2543-9. doi: 10.3748/wjg.v19.i16.2543.
18
- 453 42. Murakami T, Baron RL, Peterson MS. Liver necrosis and regeneration after
20
454 fulminant hepatitis: pathologic correlation with CT and MR findings. *Radiology*.
23
455 1996; 198:239-242. doi:10.1148/radiology.198.1.8539386
25
- 456 43. Onishi H, Theisen D, Zachoval R, Reiser MF, Zech CJ. Intrahepatic diffuse
27
457 periportal enhancement patterns on hepatobiliary phase gadoxetate disodium-
30
458 enhanced liver MR images: Do they correspond to periportal hyperintense patterns
32
459 on T2-weighted images? *Medicine (Baltimore)*. 2019; 98:e14784. doi:
35
460 10.1097/MD.00000000000014784.
37
- 461 44. Martin DR, Seibert D, Yang M, Salman K, Frick MP. Reversible heterogeneous
40
462 arterial phase liver perfusion associated with transient acute hepatitis: findings on
42
463 gadolinium-enhanced MRI. *J Magn Reson Imaging*. 2004; 20:838-842.
45
464 doi:10.1002/jmri.20192
47
- 465 45. Marzola P, Maggioni F, Vicinanza E, Daprà M, Cavagna FM. Evaluation of the
49
466 hepatocyte-specific contrast agent gadobenate dimeglumine for MR imaging of
52
467 acute hepatitis in a rat model. *J Magn Reson Imaging*. 1997; 7:147-152.
54
468 doi:10.1002/jmri.1880070121.
57
58
59
60
61
62
63
64
65

- 469 46. Dioguardi Burgio M, Bruno O, Agnello F, Torrisi C, Vernuccio F, Cabibbo G, et al.
1
2
470 The cheating liver: imaging of focal steatosis and fatty sparing. *Expert Rev*
3
4
471 *Gastroenterol Hepatol.* 2016; 10:671-8. doi: 10.1586/17474124.2016.1169919.
5
6
472 47. Karaosmanoğlu AD, Onur MR, Saini S, Taberi A, Karcaaltincaba M. Imaging of
7
8
473 hepatobiliary involvement in sarcoidosis. *Abdom Imaging.* 2015; 40:3330-7. doi:
9
10
11 10.1007/s00261-015-0533-6.
12
13
474 48. Ganeshan D, Menias CO, Lubner MG, Pickhardt PJ, Sandrasegaran K, Bhalla S.
14
15
475 *Sarcoidosis from Head to Toe: What the Radiologist Needs to Know.*
16
17
476 *Radiographics.* 2018; 38:1180-200. doi: 10.1148/rg.2018170157.
18
19
477 49. Jung G, Brill N, Poll LW, Koch JA, Wettstein M. MRI of hepatic sarcoidosis: large
20
21
478 confluent lesions mimicking malignancy. *AJR Am J Roentgenol.* 2004; 183:171-3.
22
23
479 doi: 10.2214/ajr.183.1.1830171.
24
25
480 50. Masuda K, Takenaga S, Morikawa K, Kano A, Ojiri H. Hepatic sarcoidosis with
26
27
481 atypical radiological manifestations: A case report. *Radiol Case Rep.* 2018; 13:936-
28
29
482 939. doi: 10.1016/j.radcr.2018.06.013..
30
31
483 51. Kim SH, Han JK, Lee KH, Won HJ, Kim KW, Kim JS, et al. Abdominal amyloidosis:
32
33
484 spectrum of radiological findings. *Clin Radiol.* 2003; 58:610-20. doi: 10.1016/s0009-
34
35
485 9260(03)00142-9.
36
37
486 52. DeLeve LD, Valla DC, Garcia-Tsao G; American Association for the Study Liver
38
39
487 Diseases. Vascular disorders of the liver. *Hepatology.* 2009; 49:1729-64. doi:
40
41
488 10.1002/hep.22772..
42
43
489 53. Valla DC. Budd-Chiari syndrome/hepatic venous outflow tract obstruction. *Hepatol*
44
45
490 *Int.* 2018; 12:168-180. doi: 10.1007/s12072-017-9810-5.
46
47
491 54. Buscarini E, Gandolfi S, Alicante S, Londoni C, Manfredi G. Liver involvement in
48
49
492 hereditary hemorrhagic telangiectasia. *Abdom Radiol (NY).* 2018; 43:1920-1930.
50
51
493 doi: 10.1007/s00261-018-1671-4.
52
53
494
54
55
56
57
58
59
60
61
62
63
64
65

- 495 55. Wu JS, Saluja S, Garcia-Tsao G, Chong A, Henderson KJ, White RI Jr. Liver
1 involvement in hereditary hemorrhagic telangiectasia: CT and clinical findings do
496 2 not correlate in symptomatic patients. *AJR Am J Roentgenol.* 2006; 187:W399-
3 4
497 5 W405. doi:10.2214/AJR.05.1068
6
498 7
8
9
499 10 56. Brancatelli G, Vilgrain V, Federle MP, Hakime A, Lagalla R, Iannaccone R, et al.
11
1500 12 Budd-Chiari syndrome: spectrum of imaging findings. *AJR Am J Roentgenol.* 2007;
13
14 188:W168-76. doi: 10.2214/AJR.05.0168.
1501 15
16
1502 17 57. Chung YE, Kim MJ, Park YN, Choi JY, Pyo JY, Kim YC, et al. Varying appearances
18
19 of cholangiocarcinoma: radiologic-pathologic correlation. *Radiographics.* 2009;
503 20
21 29:683-700. doi: 10.1148/rg.293085729.
504 22
23
24 25 58. Schöllkopf C, Smedby KE, Hjalgrim H, Rostgaard K, Panum I, Vinner L, et al.
26
506 27 Hepatitis C infection and risk of malignant lymphoma. *Int J Cancer.* 2008; 122:1885-
28
29 90. doi: 10.1002/ijc.23416.
30
31
508 32 59. Tomasian A, Sandrasegaran K, Elsayes KM, Shanbhogue A, Shaaban A, Menias
33
34 CO. Hematologic malignancies of the liver: spectrum of disease. *Radiographics.*
509 35
36 2015; 35:71–86. doi:10.1148/rg.351130008
37
38
39 40 60. Rajesh S, Bansal K, Sureka B, Patidar Y, Bihari C, Arora A. The imaging
41
42 conundrum of hepatic lymphoma revisited. *Insights Imaging.* 2015; 6:679-692.
43
44 doi:10.1007/s13244-015-0437-6
45
46
47 48 61. Weissleder R, Stark DD, Elizondo G, et al. MRI of hepatic lymphoma. *Magn Reson*
49
50 *Imaging.* 1988; 6:675-681. doi:10.1016/0730-725x(88)90092-6
51
52
53 54 62. Colagrande S, Calistri L, Grazzini G, Nardi C, Busoni S, Morana G, et al. MRI
55
56 features of primary hepatic lymphoma. *Abdom Radiol (NY).* 2018; 43:2277-2287.
57
58
59
60
61
62
63
64
65

- 519 63. Ippolito D, Porta M, Maino C, Pecorelli A, Ragusi M, Giandola T, et al. Diagnostic
1 approach in hepatic lymphoma: radiological imaging findings and literature review. J
520 Cancer Res Clin Oncol. 2020; 146:1545-1558. doi: 10.1007/s00432-020-03205-x.
2
3
4
521
5
6
522 64. Semelka RC, Nimojan N, Chandana S, Ramalho M, Palmer SL, DeMulder D, et al.
7
8
9
523 MRI features of primary rare malignancies of the liver: A report from four university
10
11
12
13
14
1524 65. Sato K, Takeyama Y, Tanaka T, Fukui Y, Gonda H, Suzuki R. Fulminant hepatic
15
16
17
18
19
1526 failure and hepatomegaly caused by diffuse liver metastases from small cell lung
20
21
22
23
24
2527 carcinoma: 2 autopsy cases. Respir Investig. 2013; 51:98-102. doi:
26
27
28
29
30
31
32
33
34
35
36
37
38
39
40
41
42
43
44
45
46
47
48
49
50
51
52
53
54
55
56
57
58
59
60
61
62
63
64
65
66. Tanaka K, Tomita H, Hisamatsu K, Hatano Y, Yoshida K, Hara A. Acute Liver
Failure Associated with Diffuse Hepatic Infiltration of Malignant Melanoma of
Unknown Primary Origin. Intern Med. 2015; 54:1361-1364.
doi:10.2169/internalmedicine.54.3428
67. Hanamornroongruang S, Sangchay N. Acute liver failure associated with diffuse
liver infiltration by metastatic breast carcinoma: A case report. Oncol Lett. 2013;
5:1250-1252. doi:10.3892/ol.2013.1165
68. Allison KH, Fligner CL, Parks WT. Radiographically occult, diffuse intrasinusoidal
hepatic metastases from primary breast carcinomas: a clinicopathologic study of 3
autopsy cases. Arch Pathol Lab Med. 2004; 128:1418-1423. doi:10.1043/1543-
2165(2004)128<1418:RODIHM>2.0.CO;2
69. Vernuccio F, Dioguardi Burgio M, Barbiera F, Cusmà S, Badalamenti G, Midiri M, et
al. CT and MR imaging of chemotherapy-induced hepatopathy. Abdom Radiol (NY).
2019; 44:3312-3324. doi: 10.1007/s00261-019-02193-y.
70. Vilgrain V., Lagadec M., Ronot M., Pitfalls in Liver Imaging. Radiology 2016; 278;
1:34-51. doi:10.1148/radiol.2015142576

545
1
546
3
4
547
6
548
8
9
10
11
12
13
14
15
16
17
18
19
20
21
22
23
24
25
26
27
28
29
30
31
32
33
34
35
36
37
38
39
40
41
42
43
44
45
46
47
48
49
50
51
52
53
54
55
56
57
58
59
60
61
62
63
64
65

71. Kang SP, Taddei T, McLennan B, Lacy J. Pseudocirrhosis in a pancreatic cancer patient with liver metastases: A case report of complete resolution of pseudocirrhosis with an early recognition and management. *World J Gastroenterol* 2008; 14:1622-1624. doi:10.3748/wjg.14.1622

16
17
18
19
20
21
22
23
24
25
26
27
28
29
30
31
32
33
34
35
36
37
38
39
40
41
42
43
44
45
46
47
48
49
50
51
52
53
54
55
56
57
58
59
60
61
62
63
64
65



Fig. 1 – 66-year-old cirrhotic woman with infiltrative HCC. Axial CT images on (a) arterial, (b) portal venous and (c) delayed phases demonstrate a large ill-defined mass (arrow) with no arterial hyperenhancement, mild washout on portal venous and delayed phases and an hyperenhancing portal vein tumor thrombus (arrowhead) with washout on portal venous phase. The tumor itself is not clearly visible due to inconsistent enhancement on arterial phase and only minimal washout on later phases.

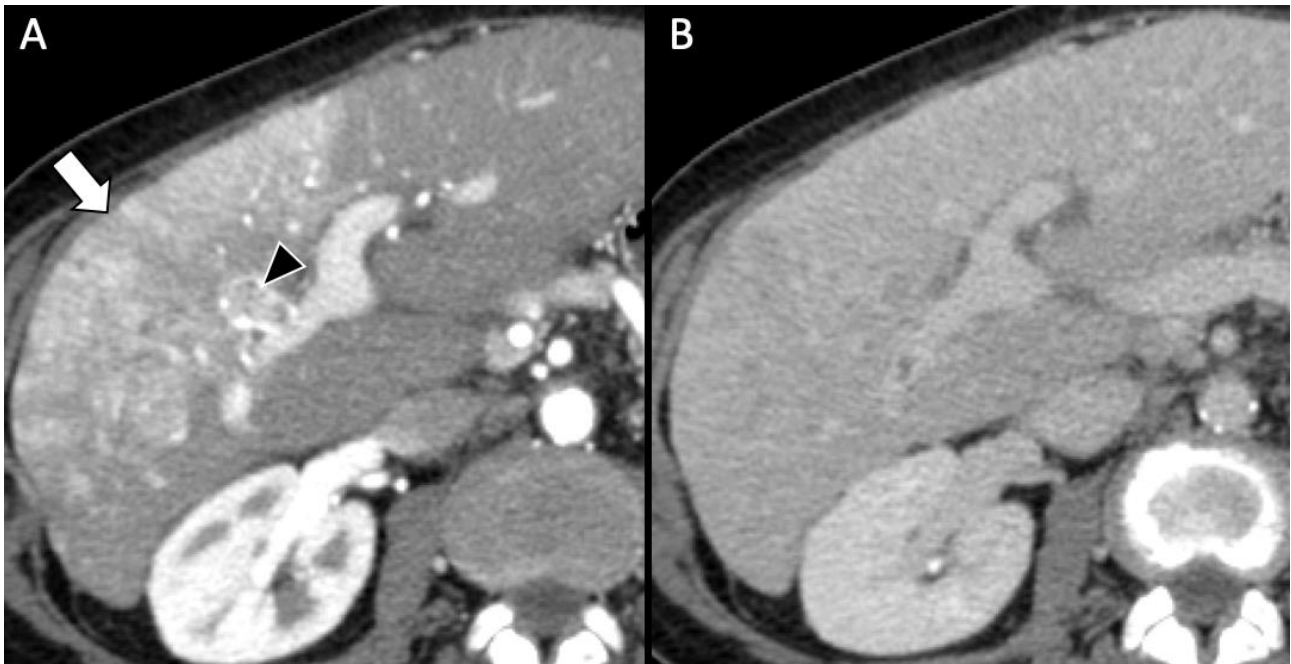


Fig. 2 – 67-year-old woman with infiltrative HCC and neoplastic tumor thrombus. Axial CT image (a) on arterial phase demonstrates an enhancing tumor thrombus (arrowhead) in the right anterior portal vein branch with the “thread and streak sign”; the malignant portal vein thrombus causes expansion of the involved portal vein branch and is adjacent to an ill-defined enhancing tumor mass (arrow) (a). Notably, the marked enhancement on arterial phase is due to both HCC and perfusion abnormalities related to portal vein thrombosis, thus overestimating the entity of the tumor mass. (b) On portal venous phase only some areas demonstrate washout within the ill-defined enhancing tumor mass.

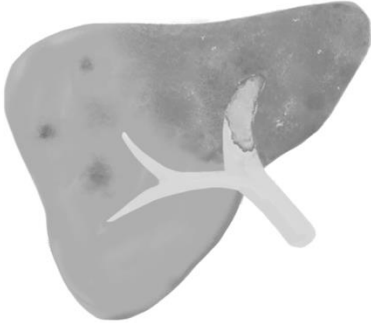
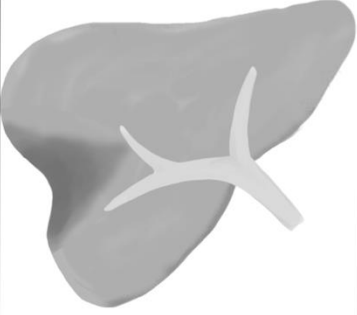
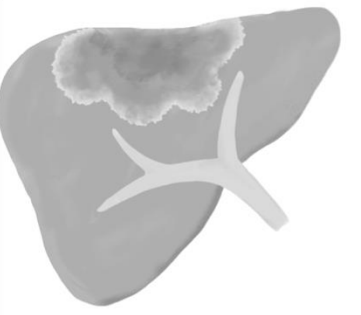
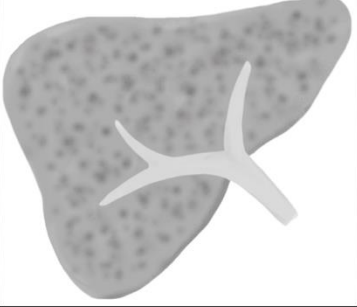
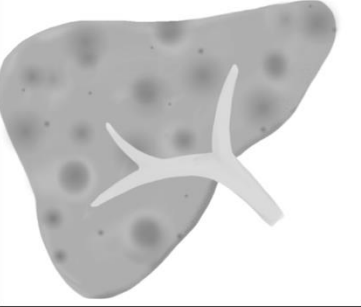


INFILTRATIVE HCC	MIMICKERS			
 <ul style="list-style-type: none"> • Ill-defined mass • Satellite nodules • Tumor thrombus 		NON-NEOPLASTIC		NEOPLASTIC
	CONFLUENT FIBROSIS		CHOLANGIOCARCINOMA	
	SARCOIDOSIS		DIFFUSE METASTASES	
	VASCULAR DISORDERS		LYMPHOMA	

Fig. 3 – Schematic representation of main imaging features of infiltrative HCC and its benign and malignant mimickers.

1
2
3
4
5
6
7
8
9
10
11
12
13
14
15
16
17
18
19
20
21
22
23
24
25
26
27
28
29
30
31
32
33
34
35
36
37
38
39
40
41
42
43
44
45
46
47
48
49
50
51
52
53
54
55
56
57
58
59
60
61
62
63
64
65

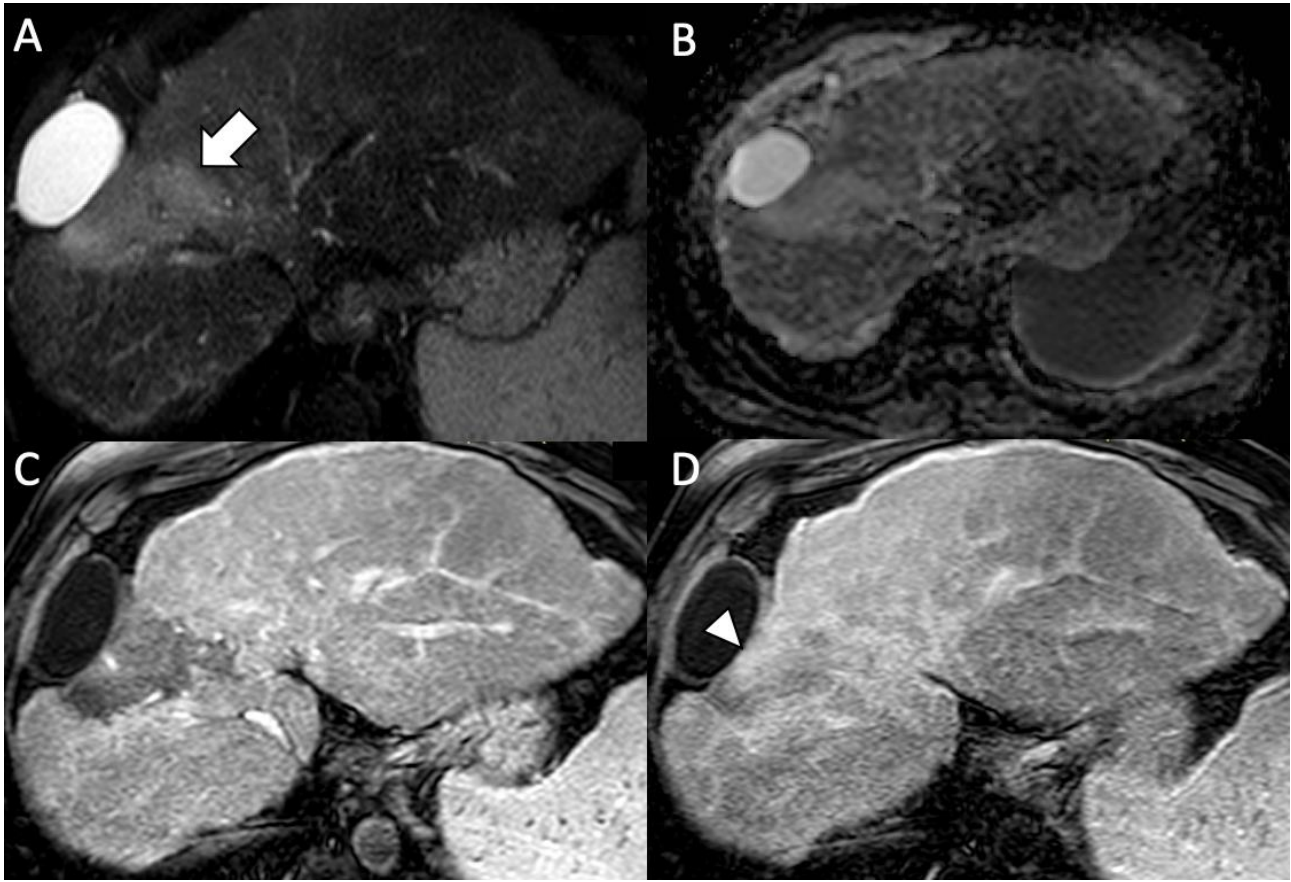


Fig. 4 – 52-year-old cirrhotic man with focal confluent fibrosis. Gadoterate meglumine MRI demonstrates on (a) T2-weighted sequence a wedge-shaped hyperintense observation (arrow) in segment VIII (b) with lack of diffusion restriction on apparent diffusion coefficient map, (c) lack of enhancement on arterial phase and (d) progressive enhancement (arrowhead) at 5-minute delayed phase.

1
2
3
4
5
6
7
8
9
10
11
12
13
14
15
16
17
18
19
20
21
22
23
24
25
26
27
28
29
30
31
32
33
34
35
36
37
38
39
40
41
42
43
44
45
46
47
48
49
50
51
52
53
54
55
56
57
58
59
60
61
62
63
64
65

16
17
18
19
20
21
22
23
24
25
26
27
28
29
30
31
32
33
34
35
36
37
38
39
40
41
42
43
44
45
46
47
48
49
50
51
52
53
54
55
56
57
58
59
60
61
62
63
64
65



Fig. 5 – 65-year-old cirrhotic man with hepatocellular carcinoma and bland thrombus. Contrast enhanced CT on (a) arterial phase shows a 2.5 cm observation (arrow) with nonrim arterial phase hyperenhancement and (b) portal venous washout, consistent with hepatocellular carcinoma. In the same patient there is also (c) a portal vein thrombus (arrowhead) that lacks any contrast enhancement on arterial phase, does not show portal vein expansion, and is distant from hepatocellular carcinoma.

1
2
3
4
5
6
7
8
9
10
11
12
13
14
15
16
17
18
19
20
21
22
23
24
25
26
27
28
29
30
31
32
33
34
35
36
37
38
39
40
41
42
43
44
45
46
47
48
49
50
51
52
53
54
55
56
57
58
59
60
61
62
63
64
65

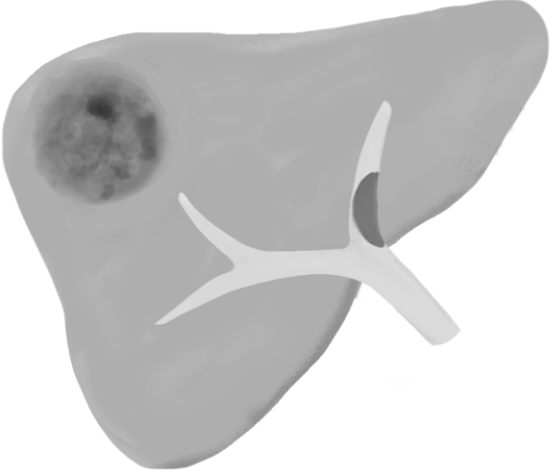
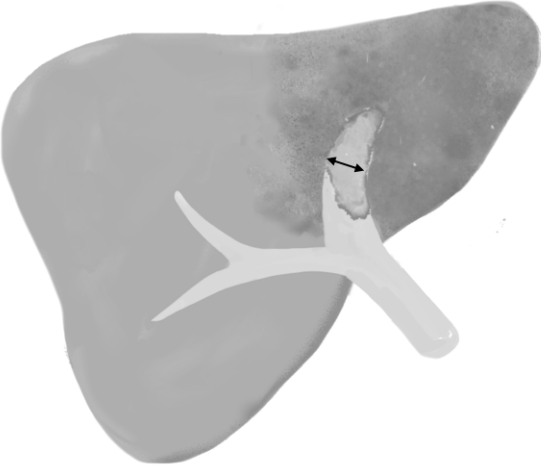
NON-NEOPLASTIC	NEOPLASTIC
	
<ul style="list-style-type: none">• No enhancement within the thrombus• No significant enlargement of portal vein• Distant from hepatocellular carcinoma	<ul style="list-style-type: none">• Enhancement within the thrombus• Enlargement of portal vein > 23 mm• Adjacent to hepatocellular carcinoma

Fig. 6 – Schematic representation of main imaging features that allow the differentiation between bland and tumor thrombosis in patients with hepatocellular carcinoma.

16
17
18
19
20
21
22
23
24
25
26
27
28
29
30
31
32
33
34
35
36
37
38
39
40
41
42
43
44
45
46
47
48
49
50
51
52
53
54
55
56
57
58
59
60
61
62
63
64
65

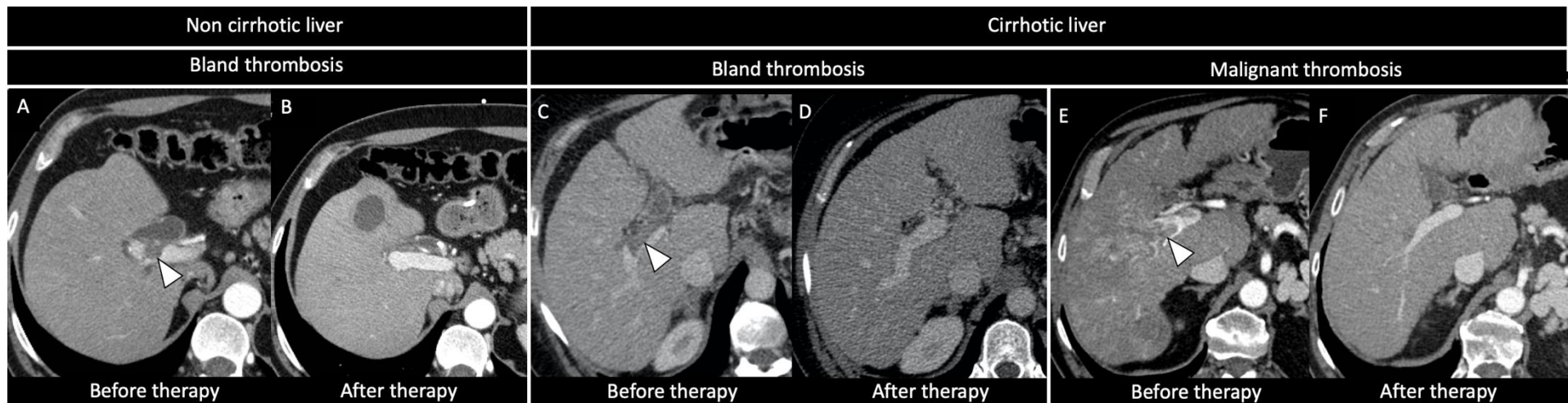


Fig. 7 – a and b: 45-year-old male-to-female transgender, in estrogenic hormone therapy with cholecystitis and bland thrombus. (a) Contrast enhanced CT on arterial phase shows a bland thrombus (arrow) in the portal vein that (b) completely regressed after anticoagulant therapy; of note, patient developed a liver abscess in segment 4 in the interval time. **c and d:** 56-year-old cirrhotic man with bland thrombus. (c) Contrast enhanced CT on portal venous phase shows a bland thrombus (arrow) in the portal vein that (d) completely regressed after anticoagulant therapy. **e and f:** 72-year-old cirrhotic man with infiltrative HCC. (e) Contrast enhanced CT on arterial phase shows an infiltrative HCC with portal vein tumor invasion (arrow) that (f) regressed after therapy with sorafenib.

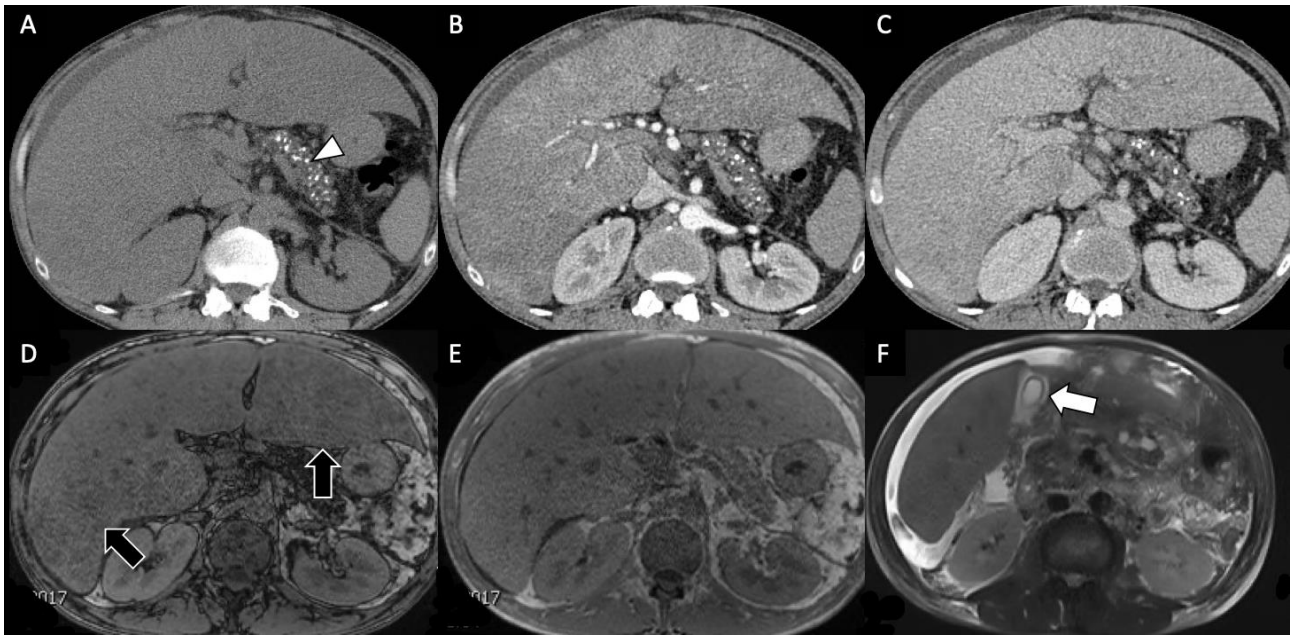
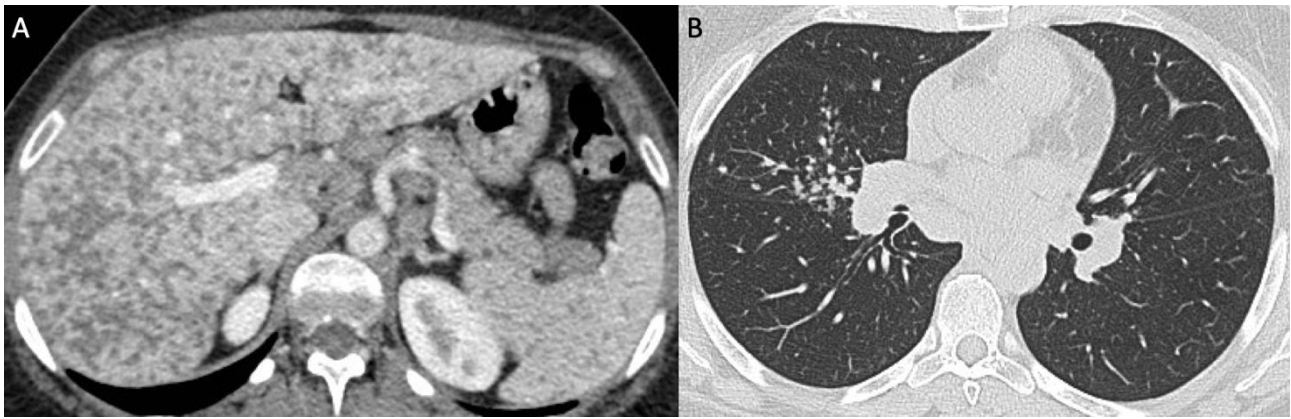


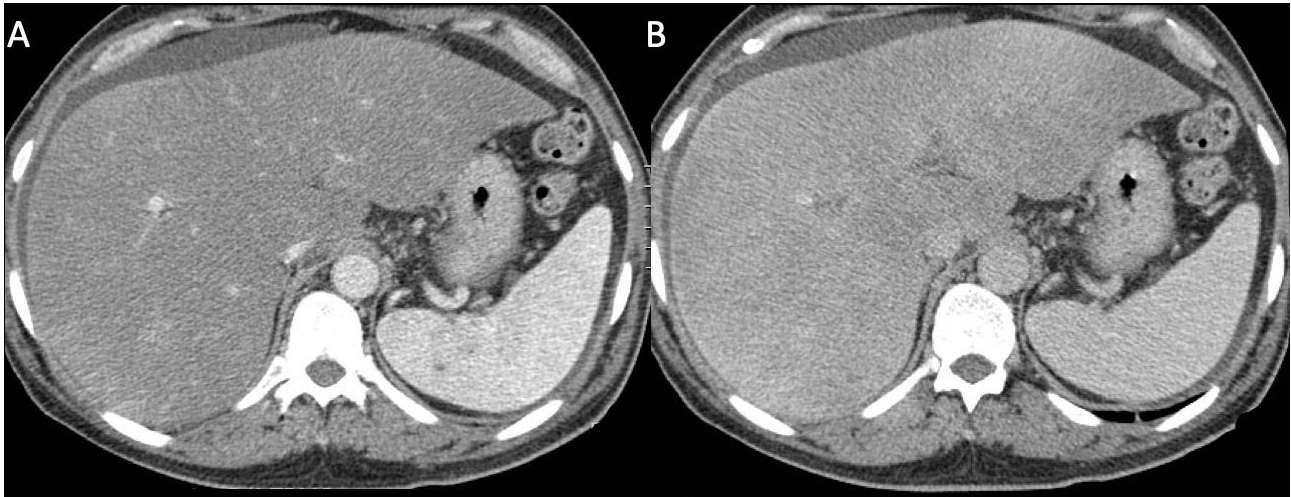
Fig. 8 – 36-year-old man with decompensated alcoholic hepatopathy and increase of cholestatic laboratory values due to acute hepatitis. Axial CT images on (a) precontrast, (b) arterial, and (c) portal venous phases show hepatomegaly with diffuse spontaneous hepatic hypoattenuation and heterogenous enhancement with ill-defined hypoattenuating areas; pancreatic calcifications (arrowhead) are also demonstrated. On MRI, dual phase sequence shows (d) signal drop (arrows) in the opposed phase compared to (e) the in-phase image. (f) Ascites and gallbladder edematous wall thickening (arrow) are demonstrated on T2-weighted image. Case courtesy of *blinded to reviewers*.



Fig. 9 – 67-year-old man with diabetes in treatment with insulin and geographical steatosis. (a) Axial CT unenhanced image showed an ill-defined hypoattenuating area (arrow) in the left lobe. Gadobenate dimeglumine-enhanced MRI demonstrated (b) marked signal drop in the opposed phase compared to (c) in-phase image, with (d) lack of enhancement on arterial phase or (e) portal venous phase with presence of undisturbed left hepatic vein and its branches traversing through the area of steatosis; (f) this area is also hypoattenuating at two hours after contrast injection; of note, in this acquisition at two hours after contrast injection, intrahepatic vessels are isointense to liver parenchyma probably due to impaired liver function and, therefore, this is similar to a transitional phase rather than an hepatobiliary phase.



1
2
3
4
5
6
7
8
9
10
11
12
13
14
15
16
17 **Fig. 10** – 48-year-old woman with sarcoidosis. (a) Axial CT image on portal venous phase
18 demonstrates multiple tiny poorly defined hypoattenuating nodules scattered throughout
19 liver and spleen. (b) Axial chest CT image in the same patient demonstrate small tiny
20
21
22
23
24
25
26
27
28
29
30
31
32
33
34
35
36
37
38
39
40
41
42
43
44
45
46
47
48
49
50
51
52
53
54
55
56
57
58
59
60
61
62
63
64
65



1
2
3
4
5
6
7
8
9
10
11
12
13
14
15
16
17 **Fig. 11** – 56-year-old man with amyloidosis; the patient was admitted for abdominal pain
18 with weight loss and asthenia for three months. Axial CT images on (a) arterial and (b)
19 portal venous phases demonstrate hepatomegaly, heterogeneously decreased
20 parenchymal attenuation on arterial phase and heterogeneous contrast enhancement with
21 diffuse low density areas scattered throughout liver parenchyma on portal venous phase.
22 These CT findings suggested diffuse infiltrative disease, so liver biopsy was performed.
23
24 The histological examination showed perisinusoidal deposits of an amorphous eosinophilic
25 material stained by Congo red stain. Biopsy results led to a final diagnosis of diffuse
26
27 amyloidosis.
28
29
30
31
32
33
34
35
36
37
38
39
40
41
42
43
44
45
46
47
48
49
50
51
52
53
54
55
56
57
58
59
60
61
62
63
64
65

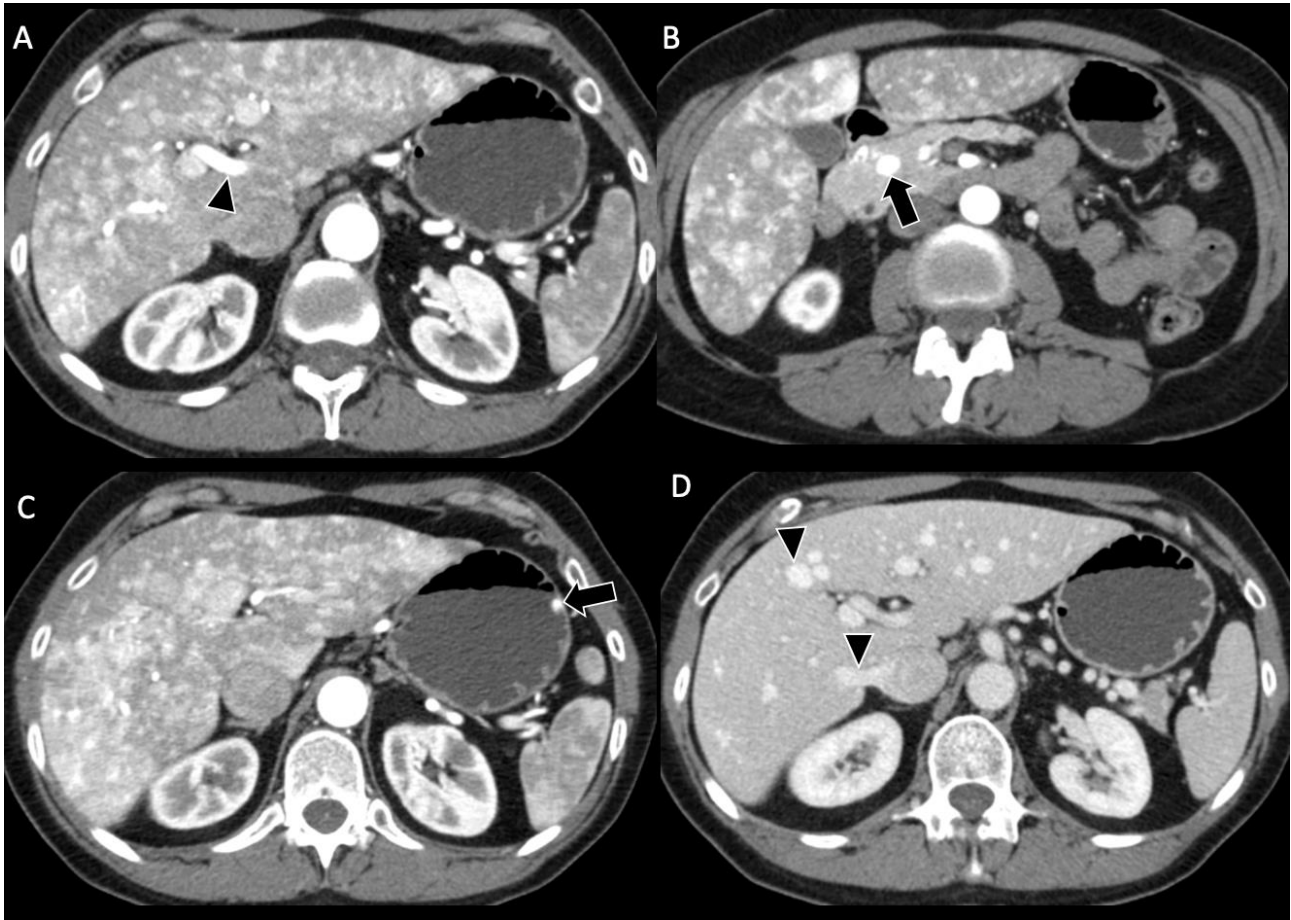
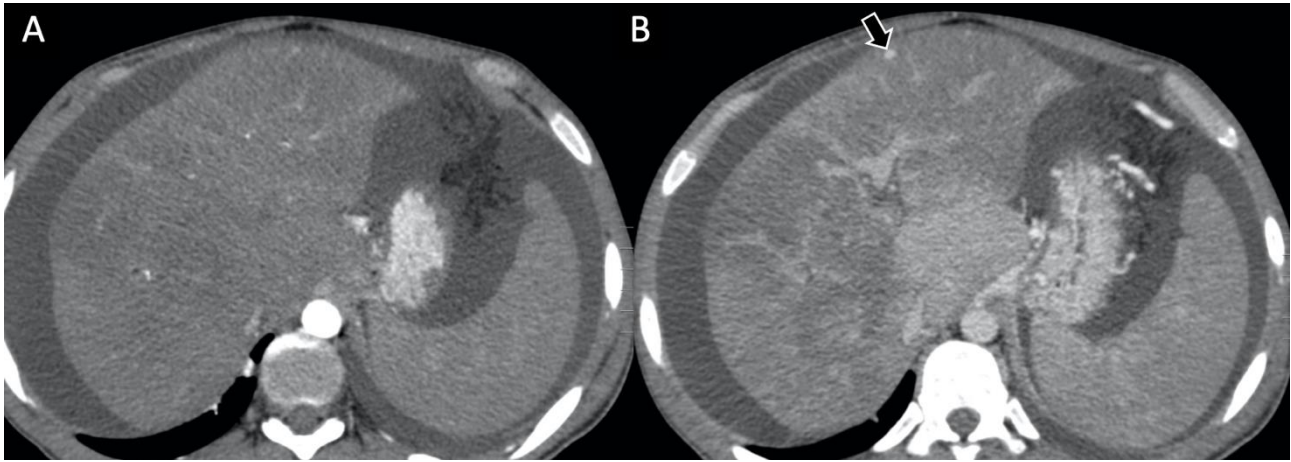


Fig. 12 – 55-year-old woman with Rendu-Osler-Weber disease; the patient was hospitalized several times for hematemesis. (a, b and c) Axial CT images on arterial phase at three different levels show a mosaic type heterogeneous perfusion pattern of the liver due to numerous arterio-portal and arterio-venous shunts, enlargement of hepatic artery (arrowhead in a), and arterio-venous shunts in the pancreatic head (arrow in b) and in the gastric wall (arrow in c). (d) Portal venous phase image demonstrates normal attenuation of the liver parenchyma and enlargement of hepatic veins (arrowheads).



1
2
3
4
5
6
7
8
9
10
11
12
13
14
15
16
17
18 **Fig. 13** – 29-year-old man with Budd-Chiari syndrome and idiopathic myelofibrosis. Axial
19 CT image on (a) arterial and (b) portal venous phases demonstrate hepatomegaly,
20
21 splenomegaly and heterogeneous hepatic and liver enhancement, with higher density of
22
23 caudate lobe compared to the remaining liver on portal venous phase due to a different
24
25 venous drainage. A small focal nodular hyperplasia-like lesion (arrow) is demonstrated in
26
27 the left lobe.
28
29
30
31
32
33
34
35
36
37
38
39
40
41
42
43
44
45
46
47
48
49
50
51
52
53
54
55
56
57
58
59
60
61
62
63
64
65

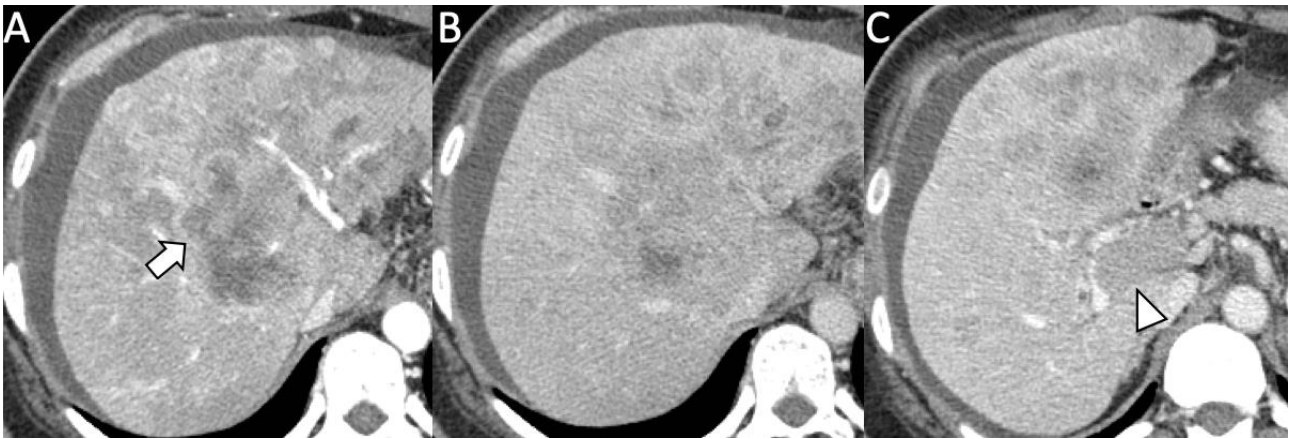


Fig. 14 – 47-year-old man with intrahepatic cholangiocarcinoma. Contrast enhanced CT image on (a) arterial phase shows a dominant mass (arrow) with peripheral enhancement, that (b) on portal venous phase demonstrates gradual centripetal central enhancement due to central fibrotic stroma. Other confluent satellite nodules are visible in the left liver. (c) Contrast enhanced CT images on portal venous phase at the level of the hepatic hilum shows the presence of tumor thrombus (arrowhead) in the portal vein, that is expanded by the tumor.

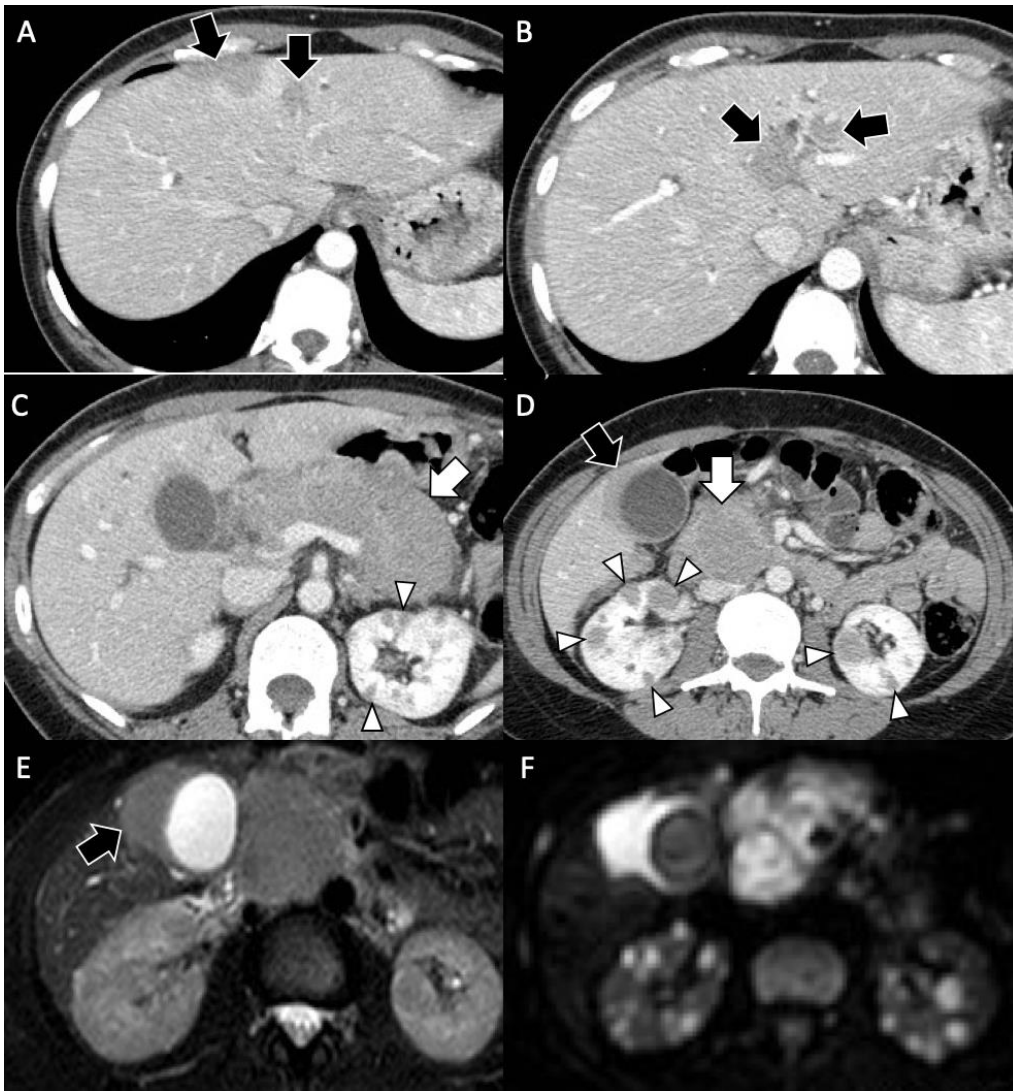


Fig. 15 – 54-year-old woman with B-cell lymphoma; symptoms at diagnosis included abdominal pain and unintentional weight loss (about 3 kilos in one week). Contrast enhanced CT images on (a, b) arterial and (c, d) portal venous phases show multiple hypoattenuating liver lesions (black arrows) alongside the portal branches, an enlarged and hypoattenuating pancreas (white arrow) as well as multiple bilateral tiny hypoattenuating renal lesions (arrowheads). Liver biopsy was performed and proved the diagnosis of B-cells lymphoma, morphologically consistent with Burkitt Lymphoma. MRI (e) on T2-weighted images show one of the lymphomatous lesions (arrow) slightly hyperintense on T2-weighted, with (f) restriction on diffusion weighted image. (f) Diffusion weighted image shows also diffusion restriction of the renal lesions.

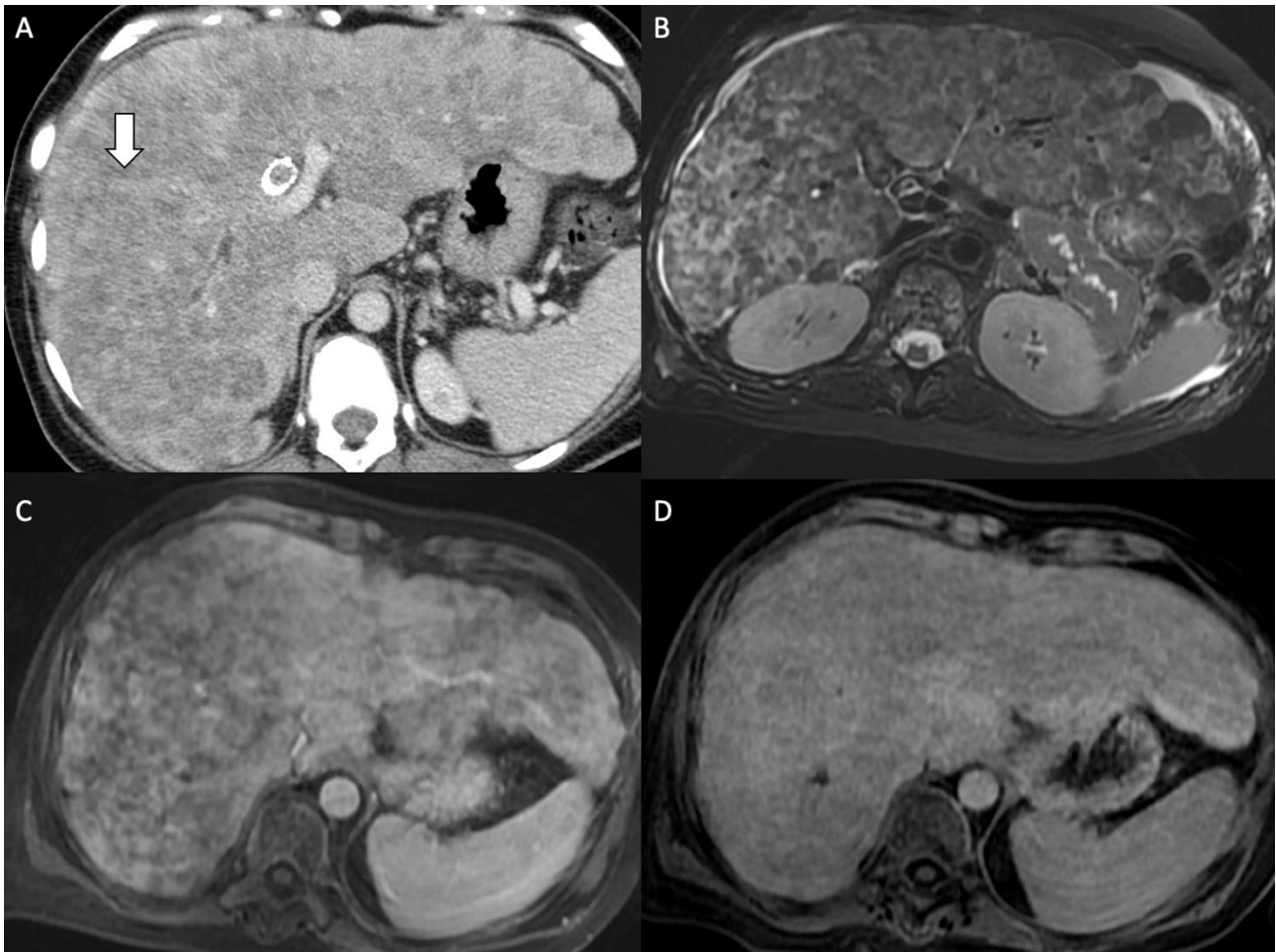
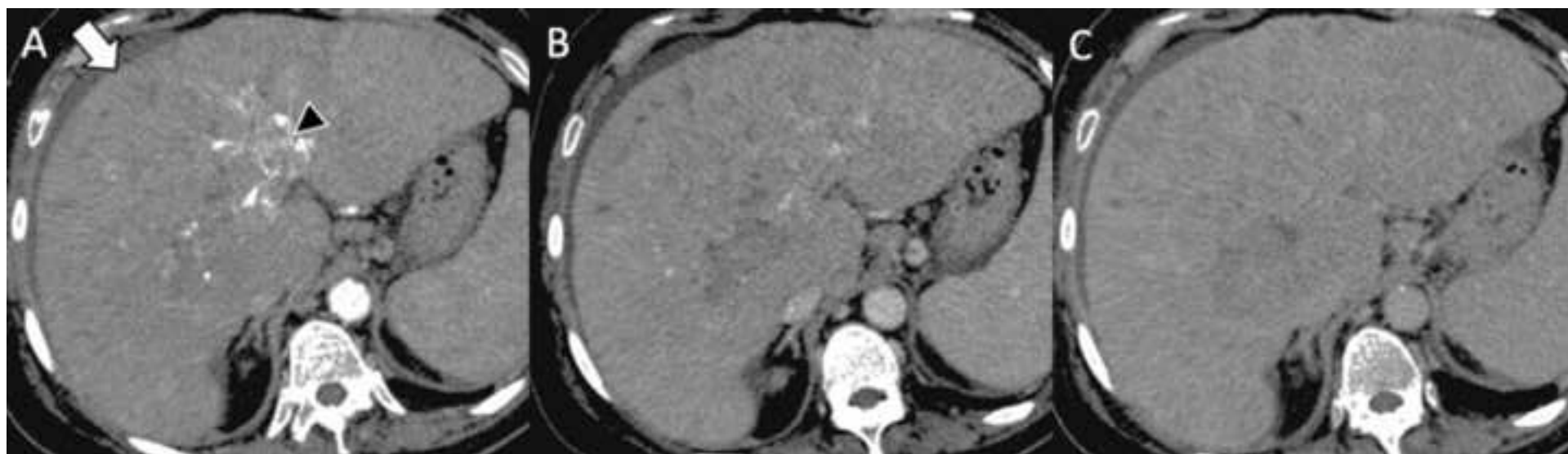
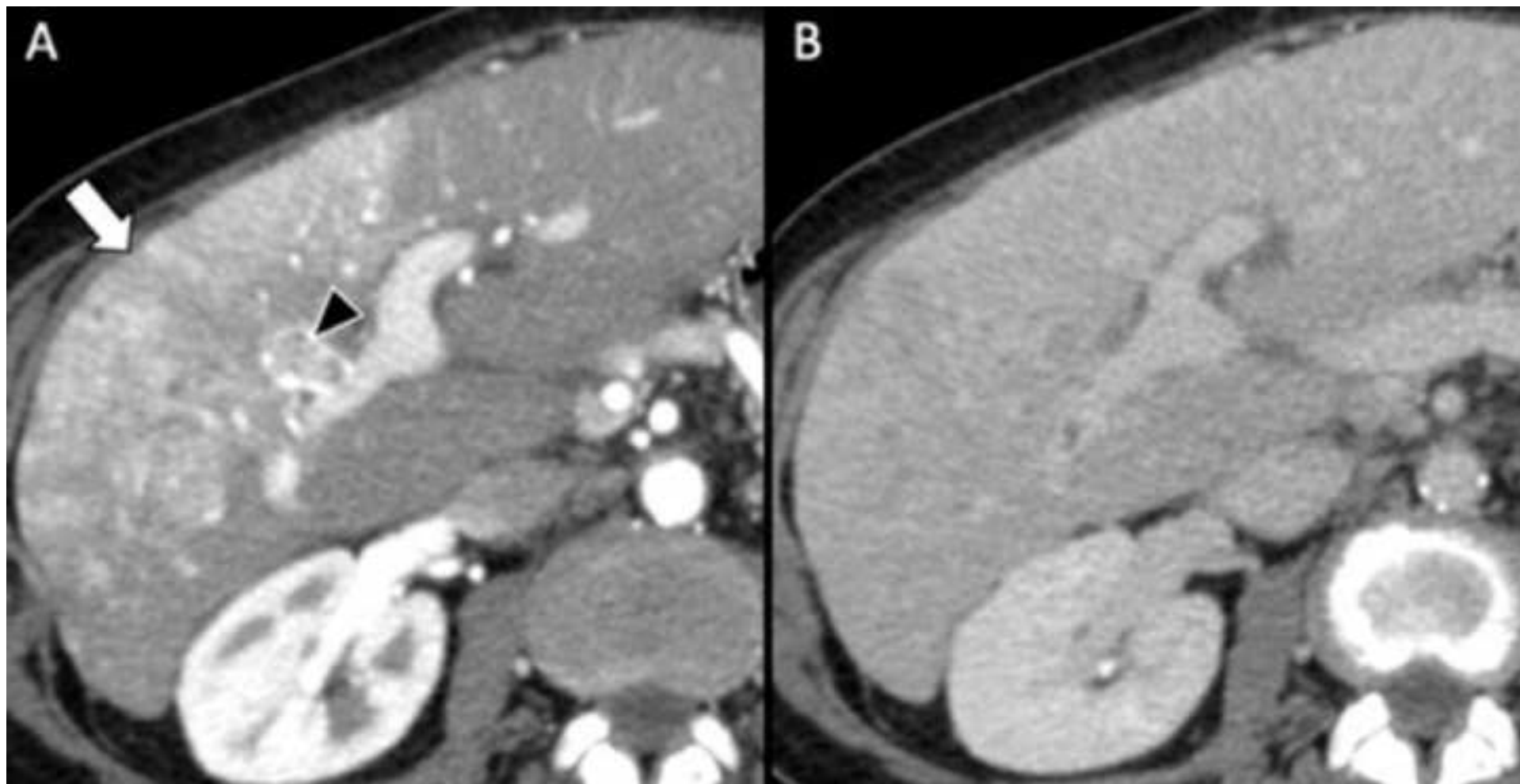

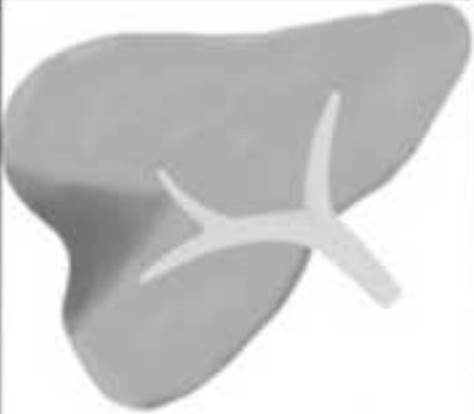
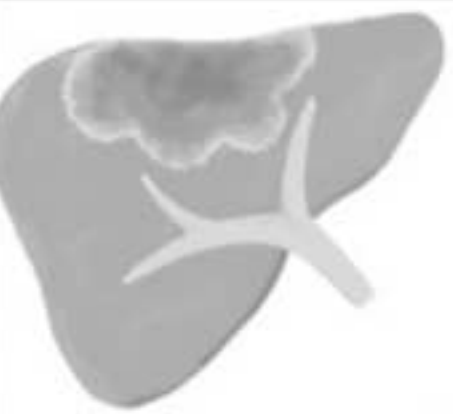
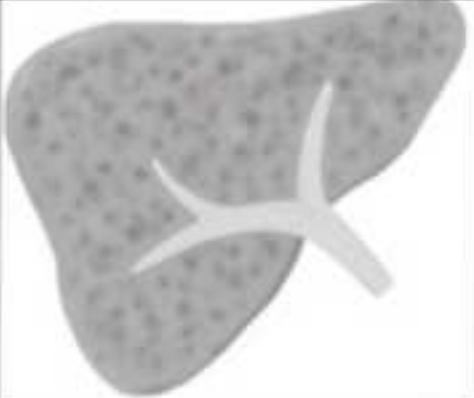
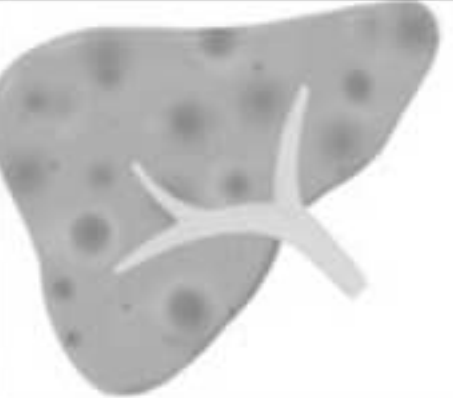
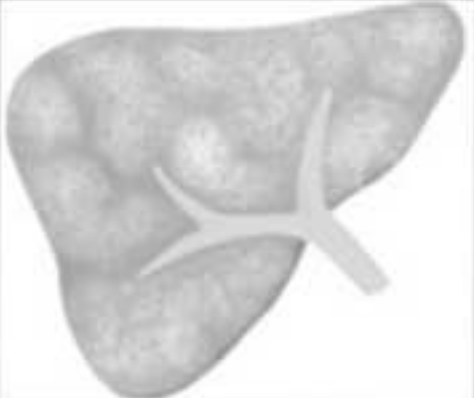
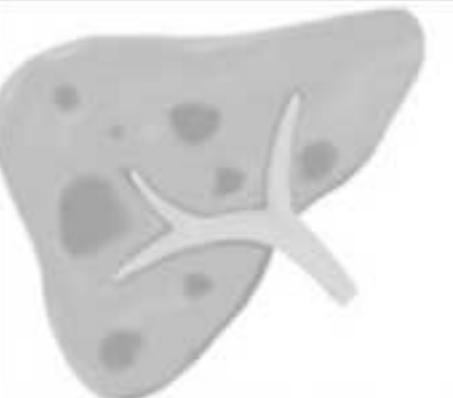
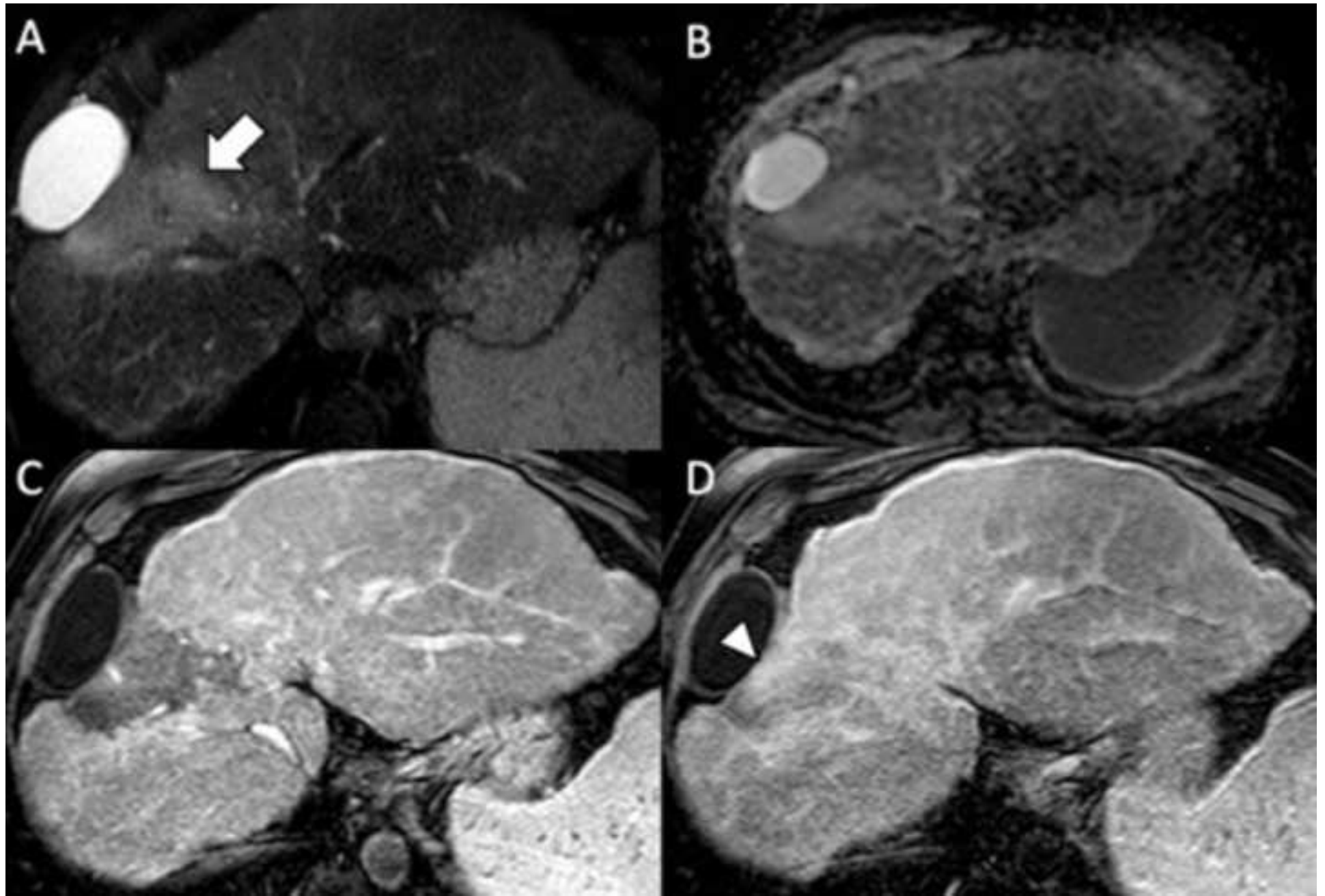


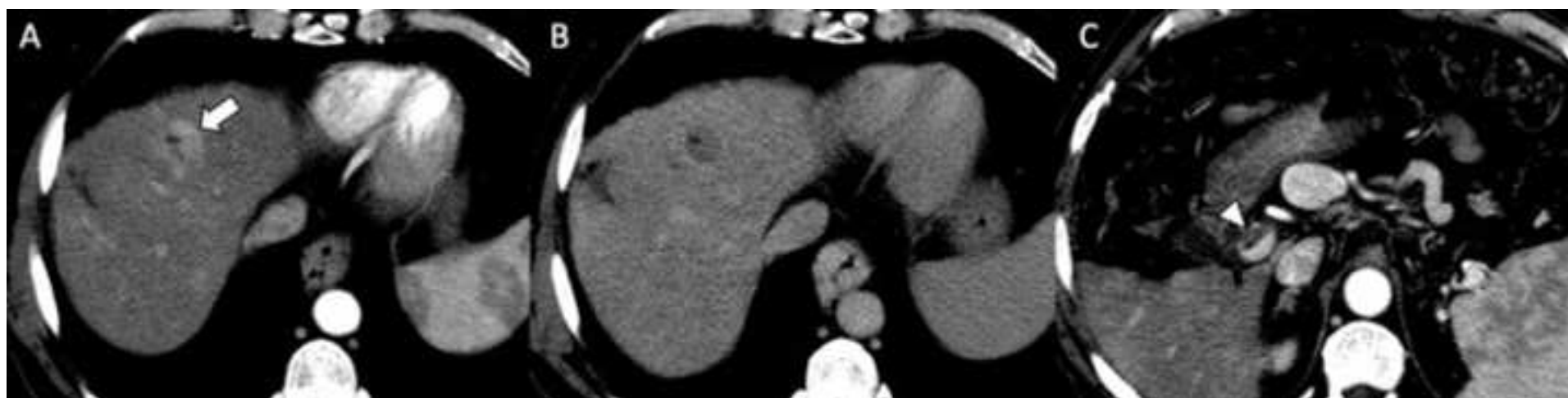
Fig. 16 – 48-year-old woman with breast carcinoma and pseudocirrhosis. (a) Contrast enhanced CT on portal venous phase shows multiple confluent hypoattenuating lesions surrounding portal vein branches (arrow) that are still patent and lobulated liver margins; the presence of multiple metastases may simulate infiltrative HCC. Gadoxetate enhanced MRI (b) on T2-weighted sequence shows a reticular pattern of hepatic parenchyma with slightly hyperintense lesions; a minimal ascites indicates worsened liver function. (c) On portal venous phase and (d) at 20 minutes after contrast injection liver parenchyma shows progressive contrast enhancement with lack of hypoattenuating lesions on hepatobiliary phase. Note isointensity of intrahepatic vessels to liver parenchyma due hepatic decompensation.

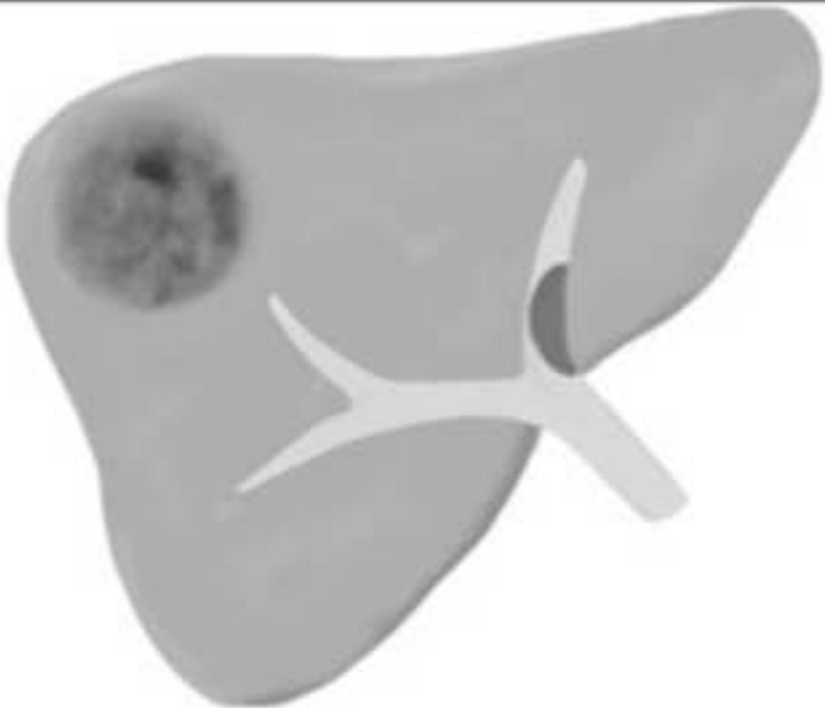
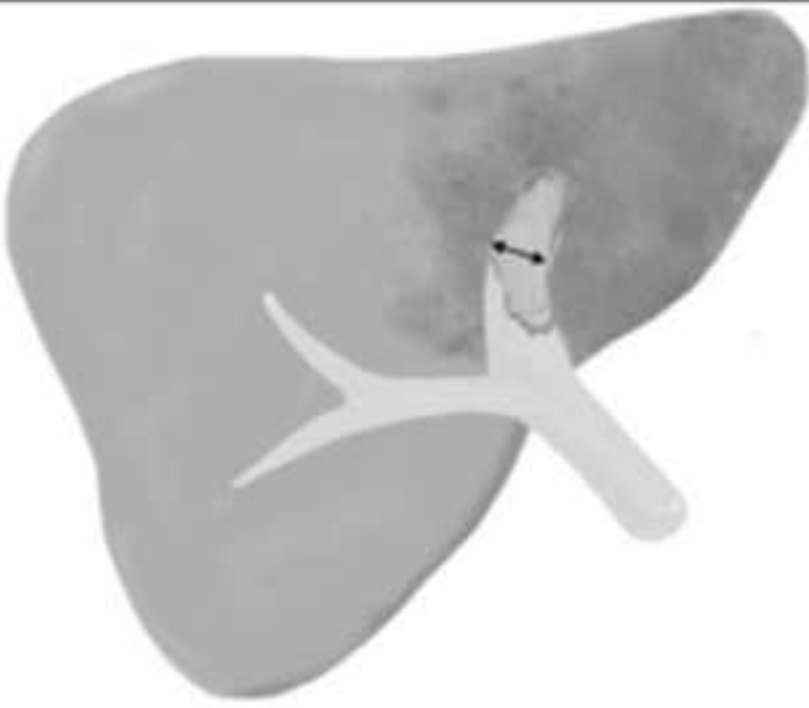


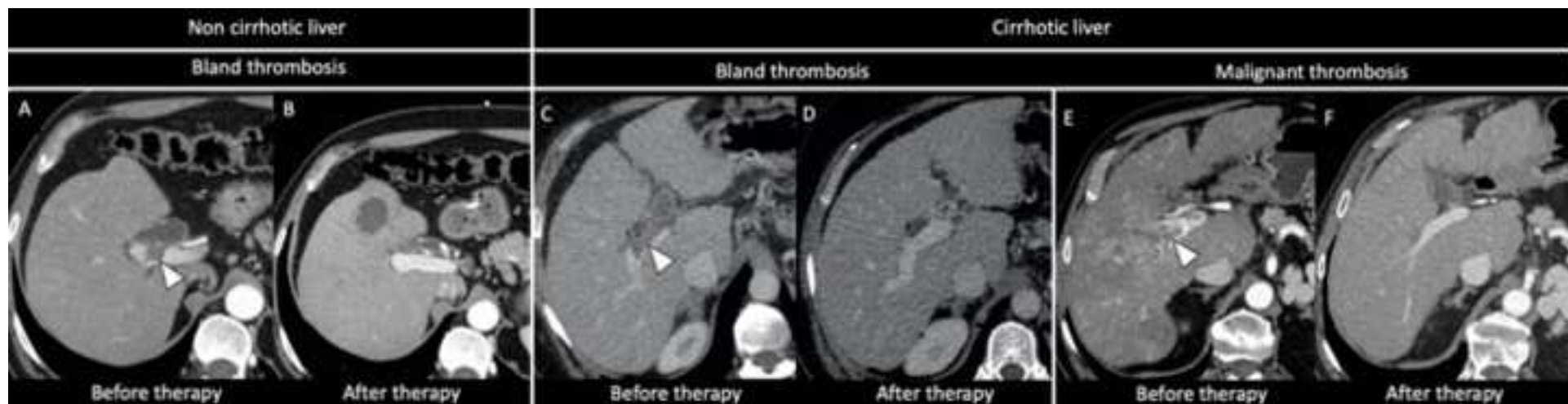


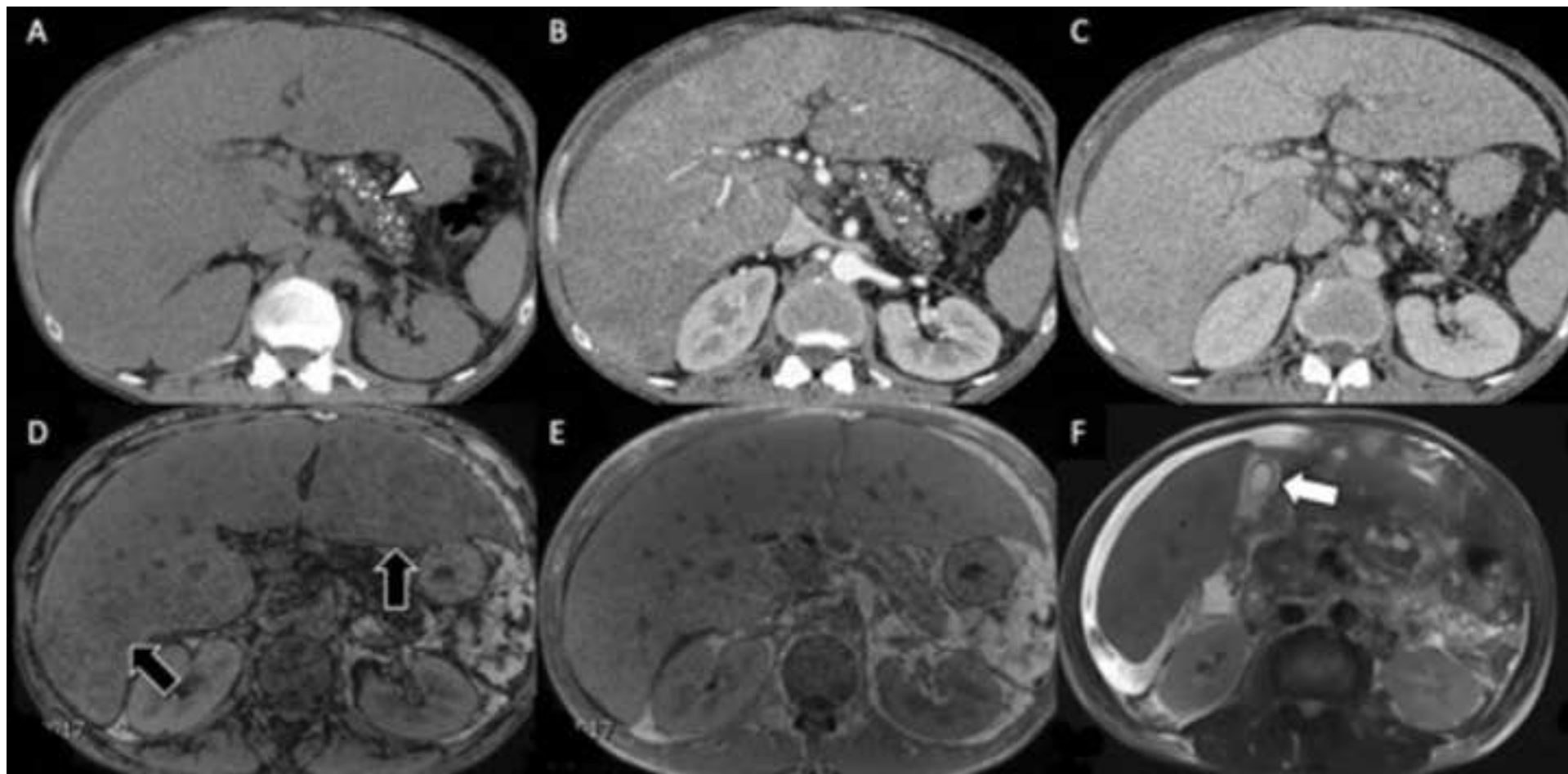
INFILTRATIVE HCC	MIMICKERS			
 <ul style="list-style-type: none"> • Ill-defined mass • Satellite nodules • Tumor thrombus 		NON-NEOPLASTIC		NEOPLASTIC
	CONFLUENT FIBROSIS		CHOLANGIOCARCINOMA	
	SARCOIDOSIS		DIFFUSE METASTASES	
VASCULAR DISORDERS		LYMPHOMA		

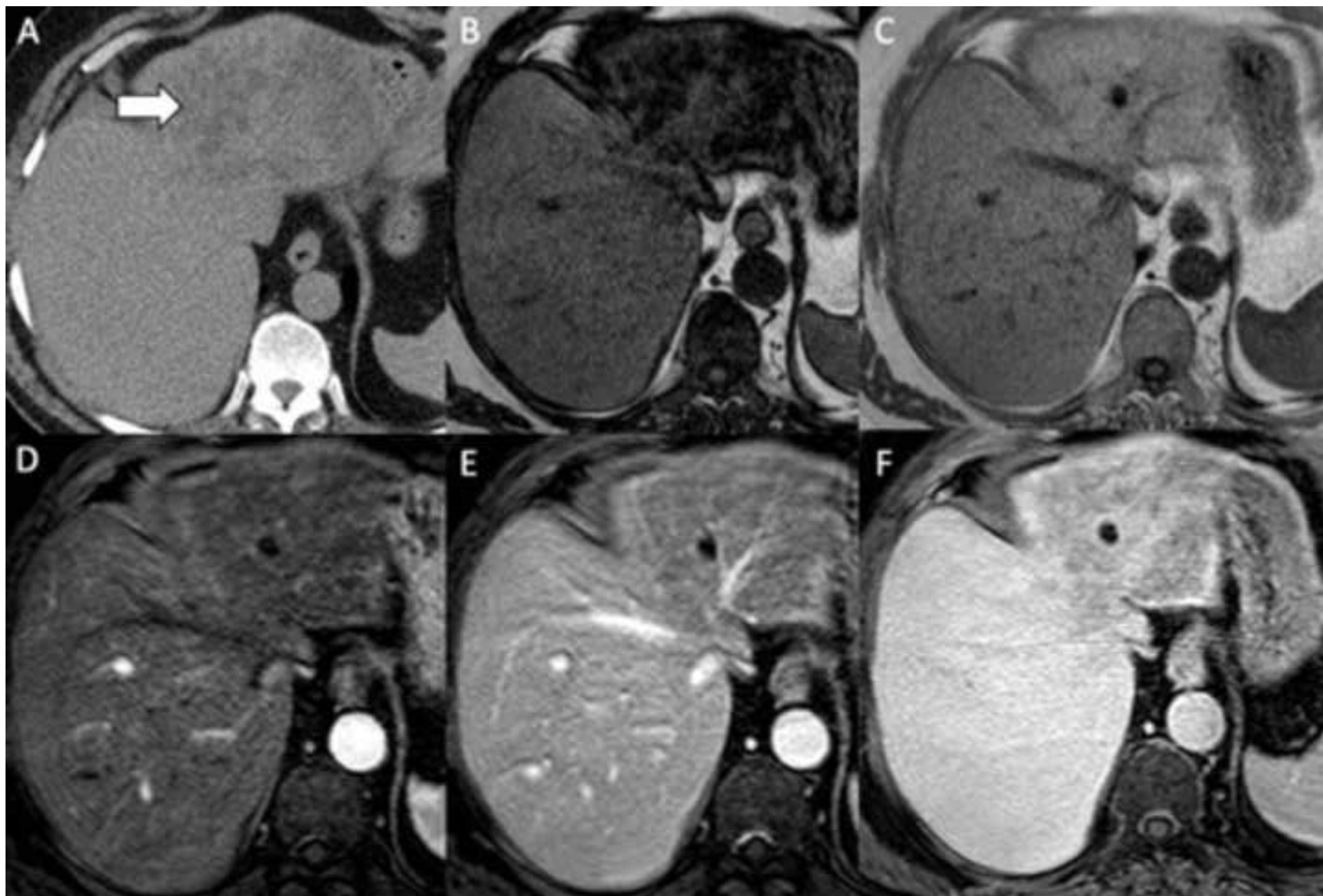


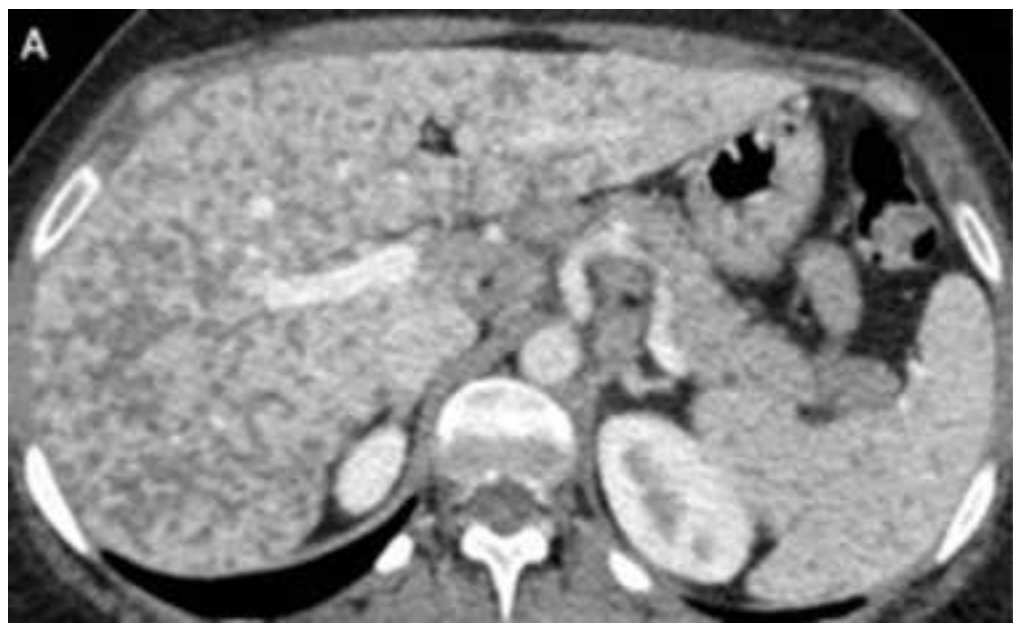


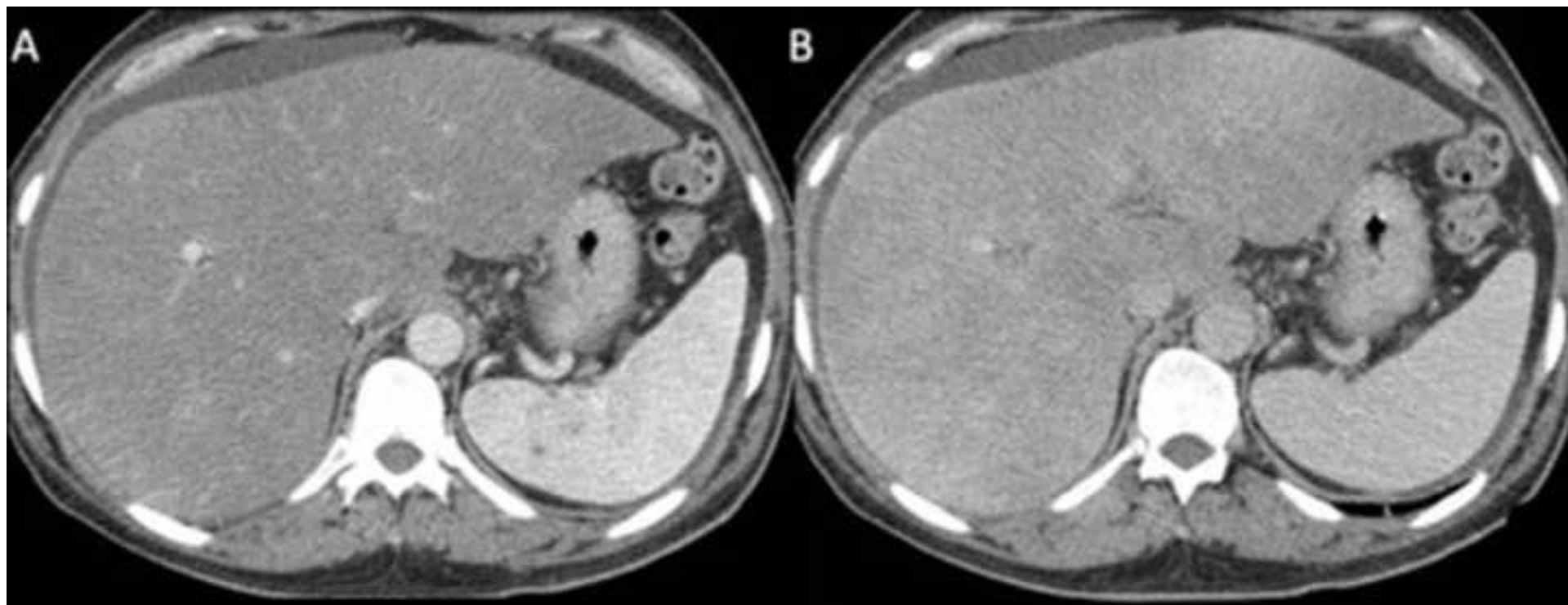
NON-NEOPLASTIC	NEOPLASTIC
	
<ul style="list-style-type: none">• No enhancement within the thrombus• No significant enlargement of portal vein• Distant from hepatocellular carcinoma	<ul style="list-style-type: none">• Enhancement within the thrombus• Enlargement of portal vein > 23 mm• Adjacent to hepatocellular carcinoma

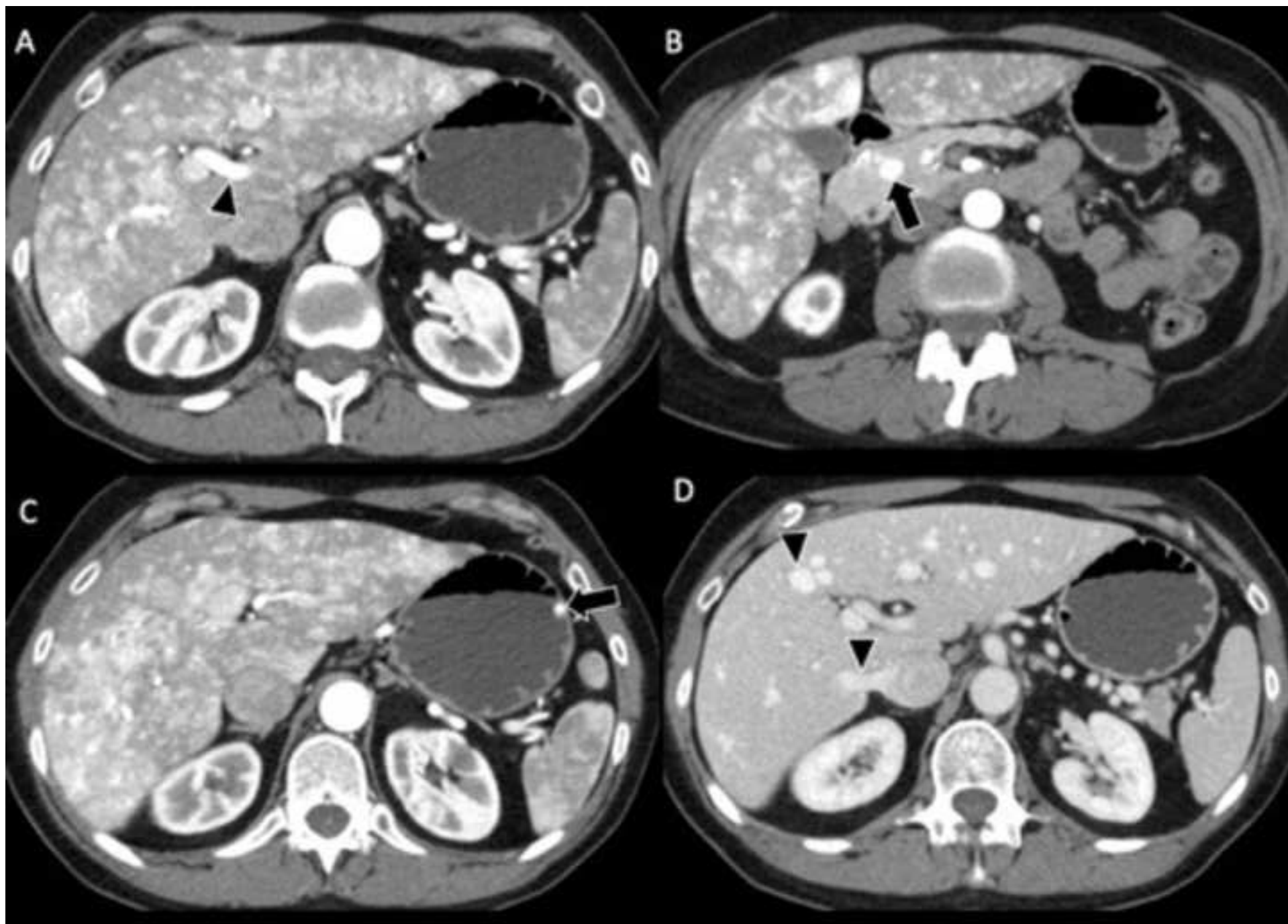


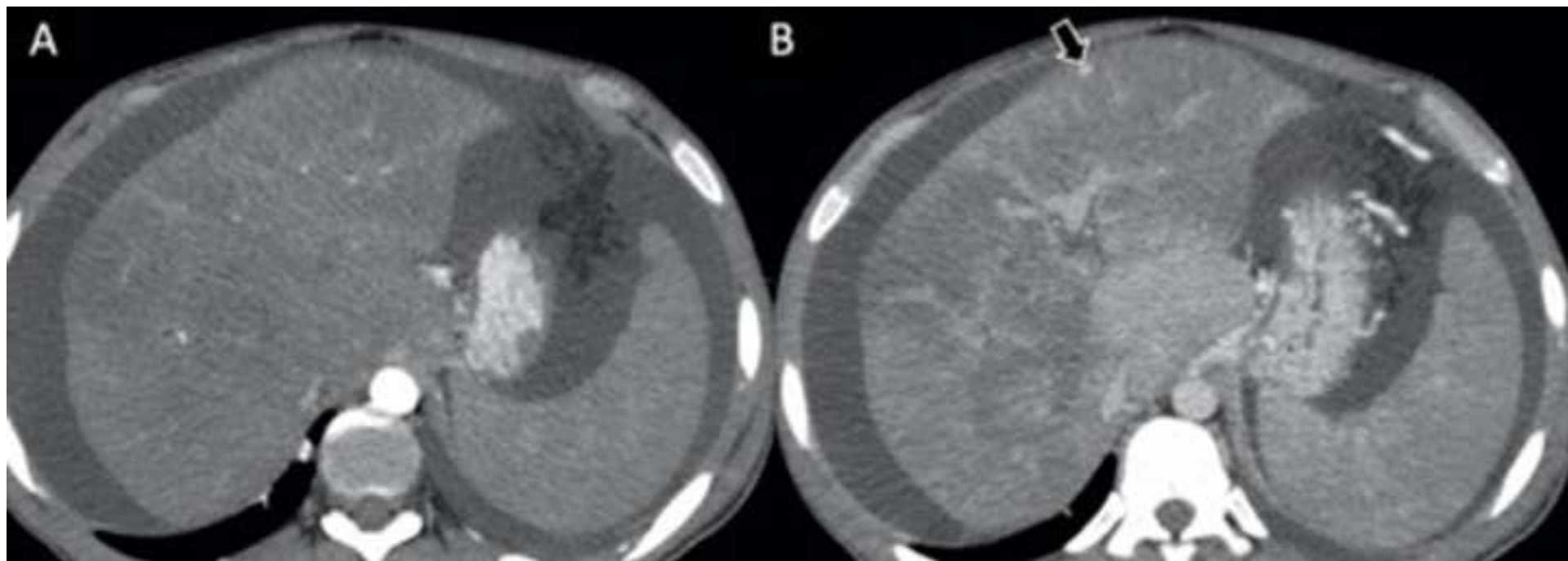


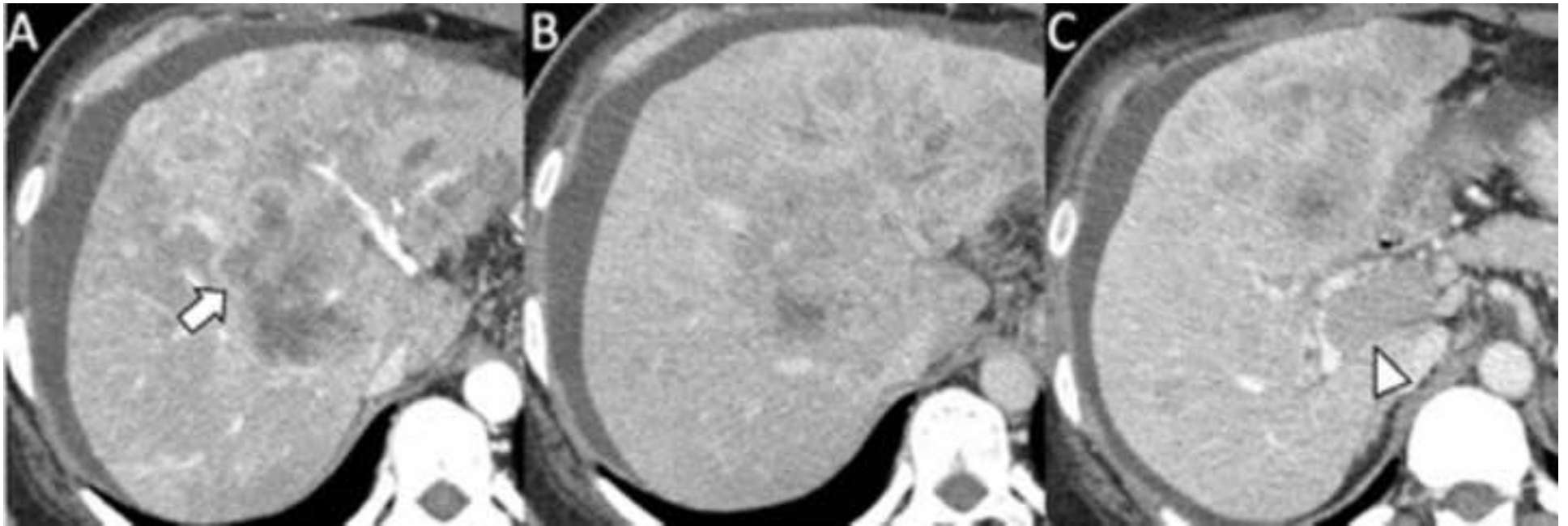




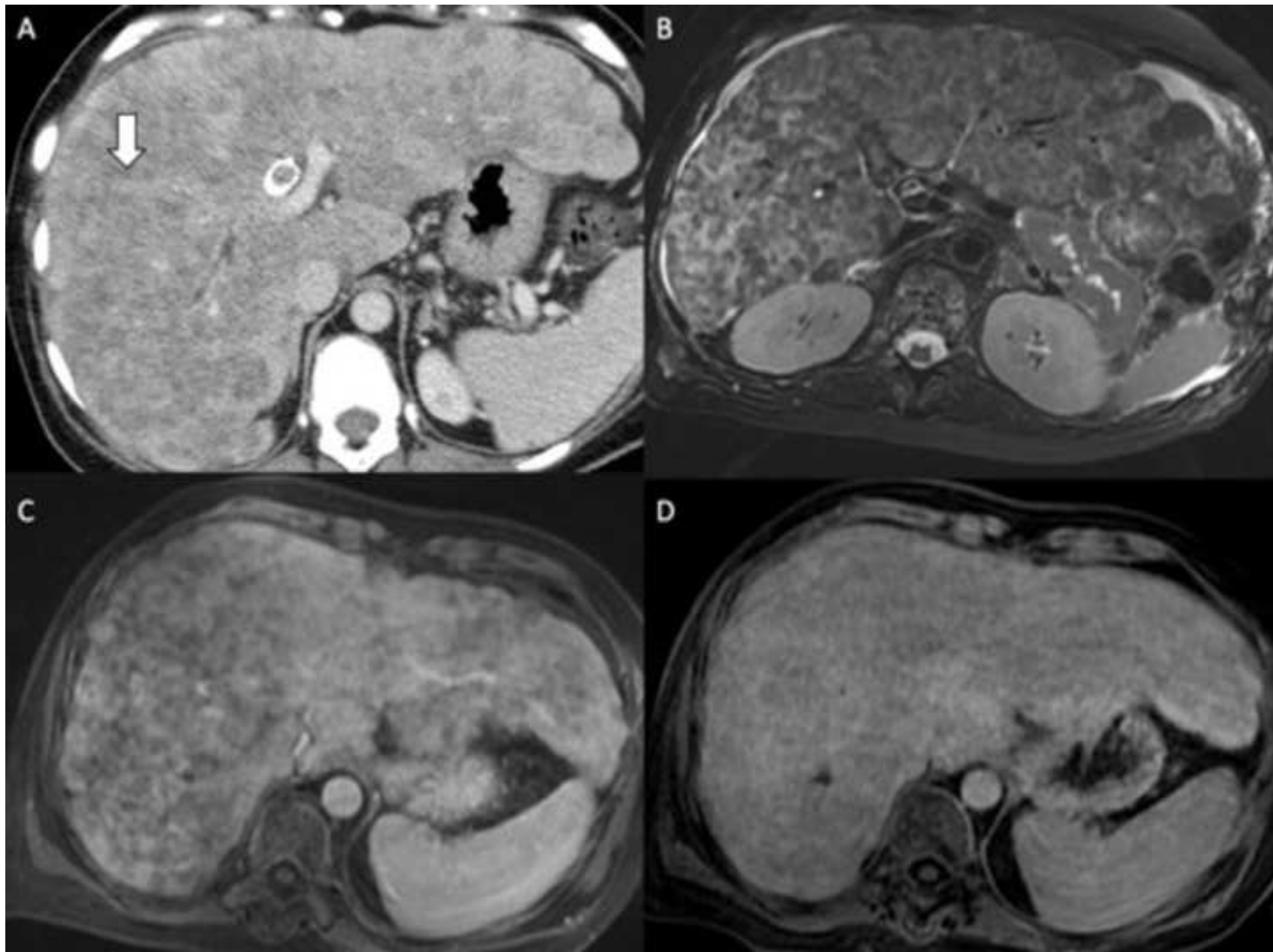












Highlights

- Infiltrative HCC appears as an ill-defined large mass with variable enhancement
- Portal vein tumor thrombosis appears as enhancing thrombus close to the main tumor
- Diagnosis of infiltrative HCC and neoplastic thrombosis may be challenging
- Many benign and malignant lesions may mimic infiltrative HCC and tumor thrombosis